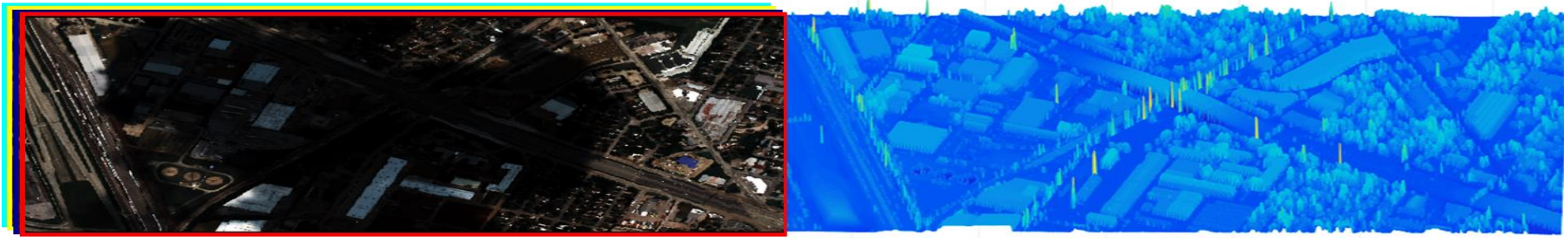

# Deep Learning for Fusion of Hyperspectral and LiDAR Remote Sensing Images for Classification


Wenzhi Liao

VITO and Ghent University-IMEC

Wenzhi.liao@ugent.be

# Ghent University

Belgium

Ghent

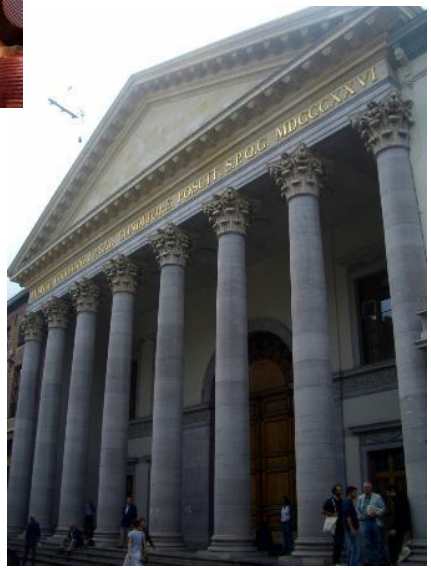

Ghent University

# VITO

- **Mission:** As independent and customer-oriented research organization, VITO (around 600 employees) provides innovative technological solutions as well as scientifically based advice and support in order to stimulate sustainable development and reinforce the economic and social fabric of Flanders.

- ***Active in Sustainable Technologies in the field of:***
  - ***Environment***
  - ***Energy***
  - ***Materials***
    - Circular economy strategic advice for companies
    - Recovery of materials from waste
    - Shaping materials
  - ***Remote sensing***

- ***More information: www.vito.be***

vito **Flemish Institute for Technological Research**

I. A comparison on feature fusion of hyperspectral and LiDAR data for classification

II. Fusion of APEX hyperspectral and LiDAR data for tree species classification

vito

GHENT UNIVERSITY

I. A comparison on feature fusion of hyperspectral and LiDAR data for classification

II. Fusion of APEX hyperspectral and LiDAR data for tree species classification

vito

GHENT UNIVERSITY

# Acknowledgements

Dr. Renbo Luo
Guangzhou University, China

Mr. Xudong Zhao
Ghent University, Belgium

# What and why hyperspectral and LiDAR data?

vito

GHENT UNIVERSITY

# What and why hyperspectral images?

Discriminate real or fake leaves

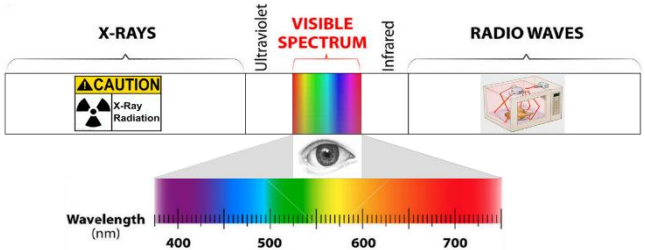


Human eyes typically respond to wavelengths

See the disease symptoms?

**Seeing is believing?**

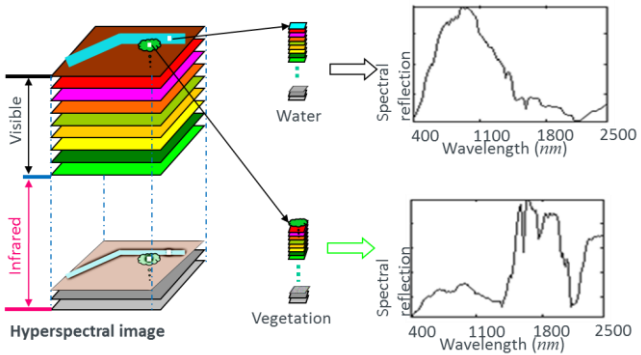


Hyperspectral imaging for material identification

# What and why hyperspectral images?

**Cancer detection**

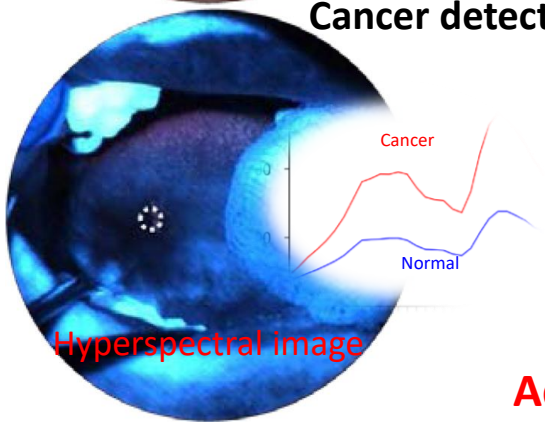


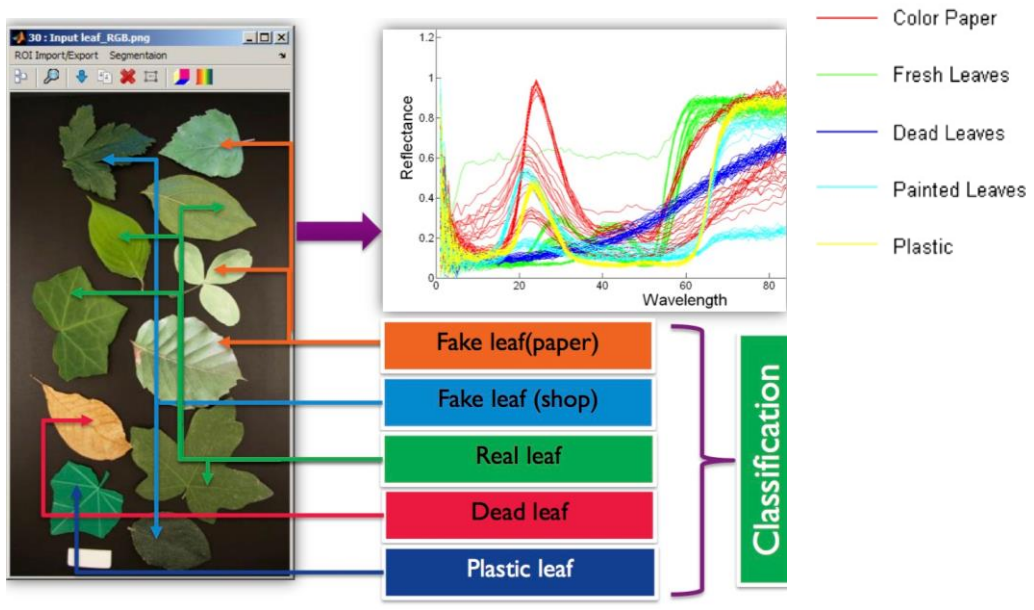


**Materials identification**

**Advanced "seeing" + analysis enable better believing**

# Applications of hyperspectral images

**Precision agriculture:** UAV + hyperspectral camera + smart algorithms

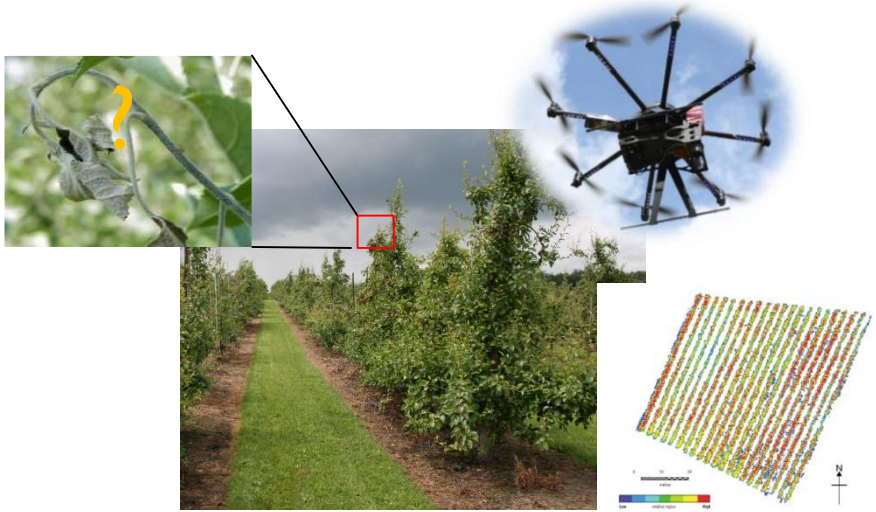

**Objective: Increase** the crop **productivity** on both quality and quantity while **reducing** the **cost**

**Forest tree mapping**

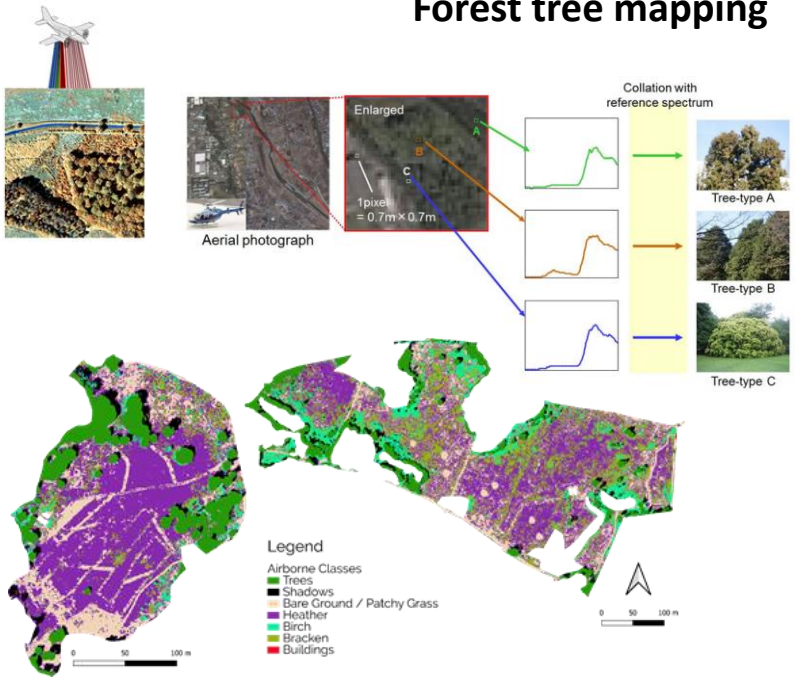

# Limitations of hyperspectral images

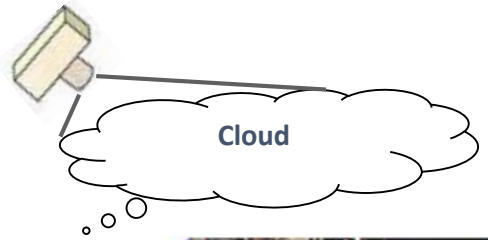


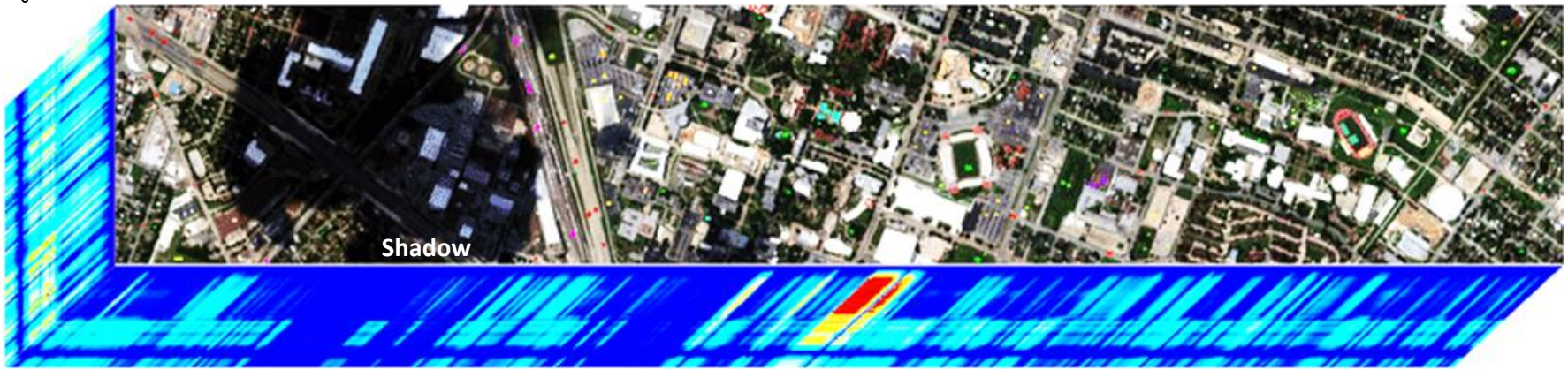


**Hyperspectral image**
is difficult to detect objects under shadow

# What and why LiDAR data?

- LiDAR stands for Light Detection and Ranging, commonly known as ***Laser Radar***
- LiDAR is not only replacing conventional sensors, but also creating new methods with unique properties that could not be achieved before

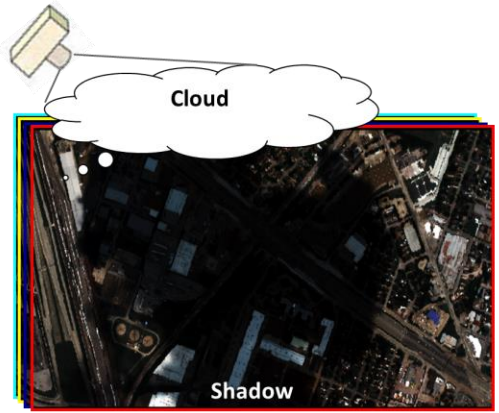


**LiDAR image** can penetrate clouds to measure the height of objects on the ground

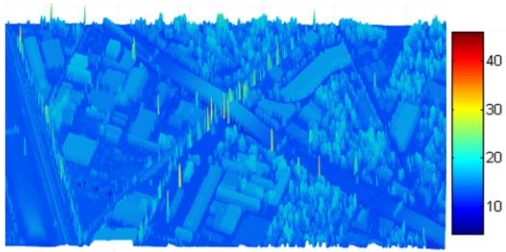

# What and why LiDAR data?

Each time the laser is pulsed:

- Laser generates an optical pulse
- Pulse is reflected off an object and returns to the system receiver
- High-speed counter measures the time of flight from the start pulse to the return pulse
- Time measurement is converted to a distance (the distance to the target and the position of the airplane is then used to determine the elevation and location)
- Multiple returns can be measured for each pulse

Everything that can be seen from the aircraft is measured

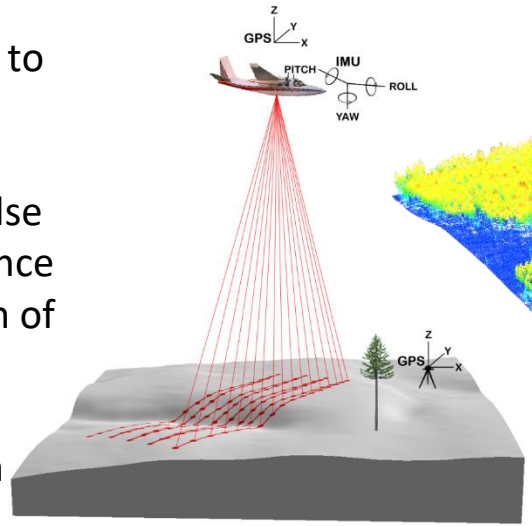


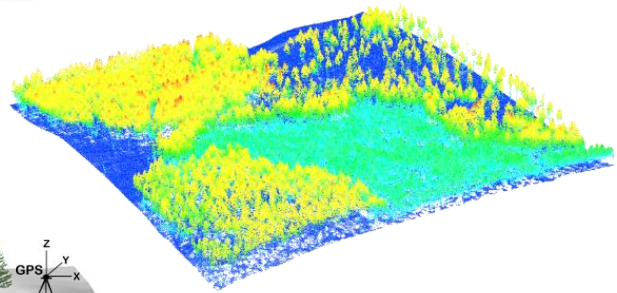

# Applications of LiDAR

**3D urban planning**

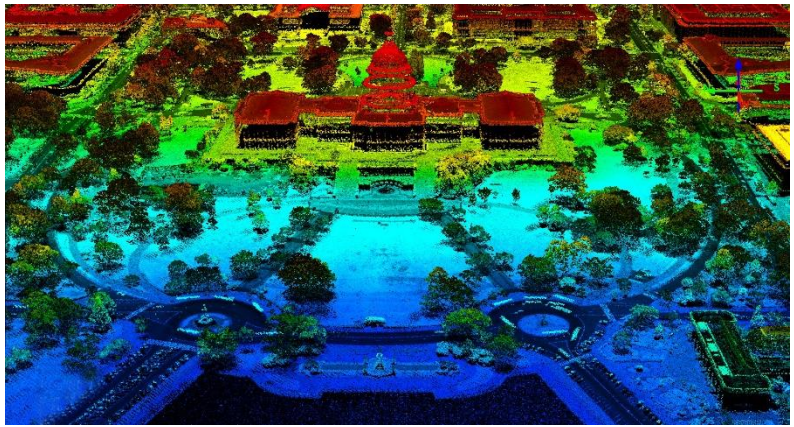

**Disaster managements**

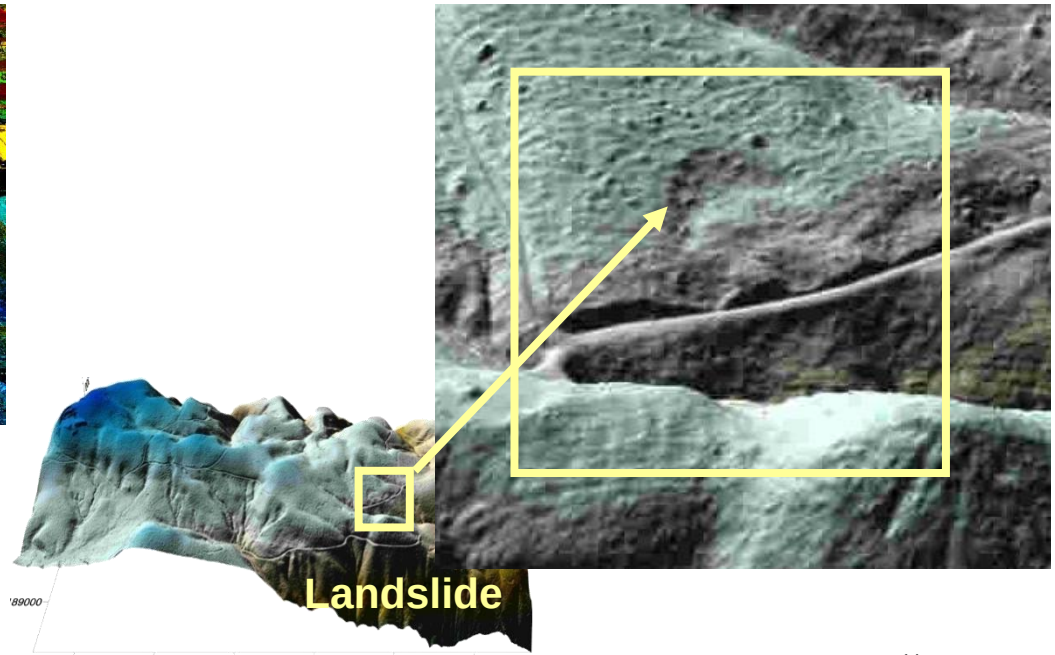

# LiDAR data

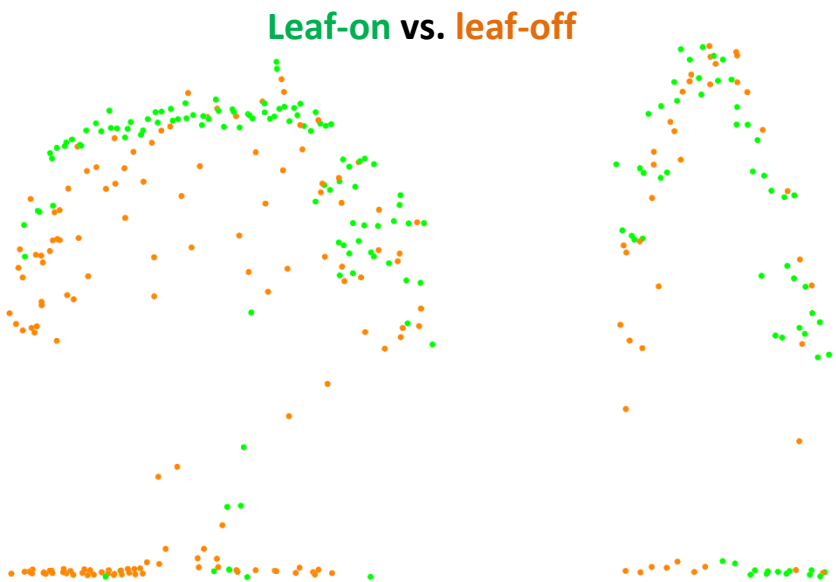


**LIDAR Derived Products**

Topographic LiDAR systems produce surface elevation x, y, z coordinate data points. There are many products that can be derived from raw point data. Most LiDAR providers can derive these products upon request:

- Digital Elevation Models (DEMs)
- Digital Terrain Models (DTMs) (bald-earth elevation data)
- Digital surface model (DSM): “top surface”

# Challenges

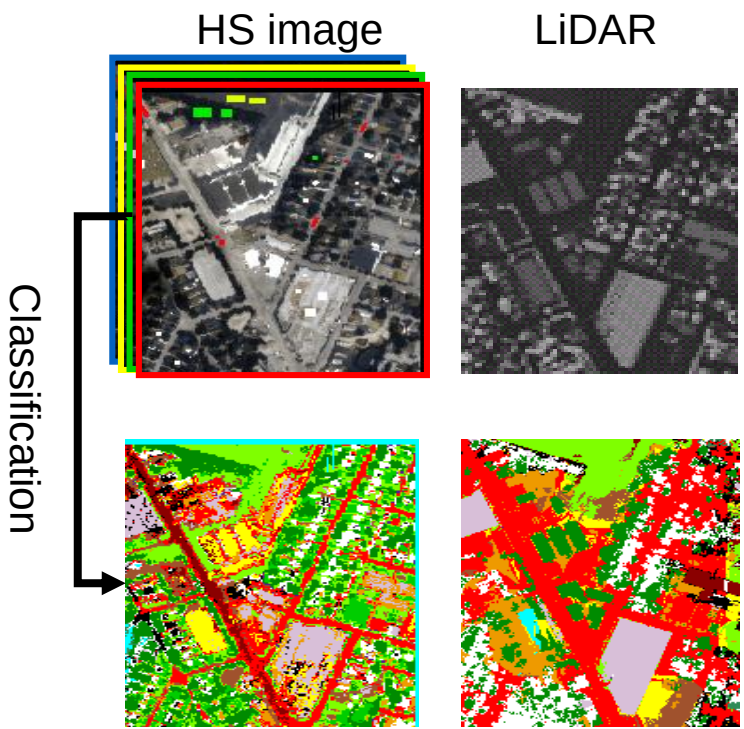


- ✓ Single data source is not enough for a reliable classification
- ✓ HS and LiDAR images provide complementary information
- ✓ How to fuse multi-sensor data?

# Methods for feature extraction

# Multi-level features

**Low-level neighborhood information**

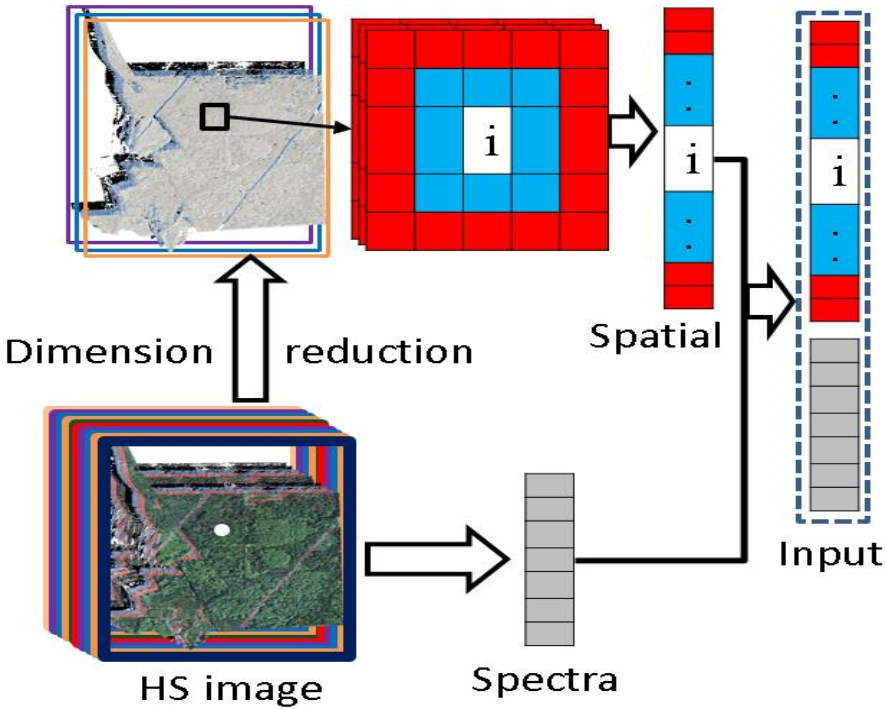


**Spectral-spatial features**

# Multi-level features

Morphological operations
(e.g., dilation and erosion)

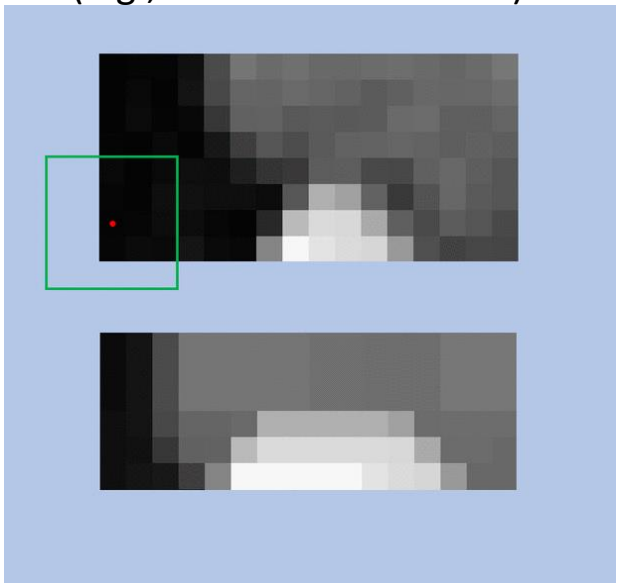

**Middle-level morphological information**

**Closing:** the combination of dilation and erosion

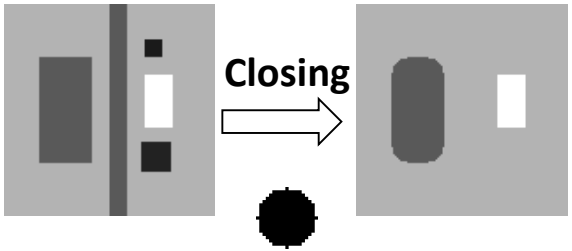


**Structure element:**

Returning the maximum/minimum value within **a moving window (structure element)**

Math. morphology to incorporate the contextual information

# Multi-level features

**Middle-level morphological information**

Morphological Closings

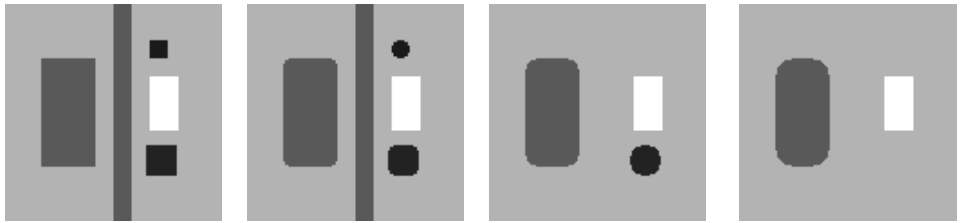

Morphological Profile

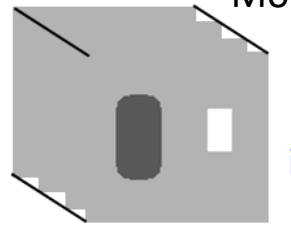

Contain spatial information (e.g., size, shape, etc.)

Size structuring element

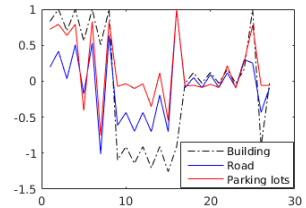

# Multi-level features

LiDAR

Objects with high elevation disappear

Openings

**Morphology**

0 1 3 5

Closings

Dark objects disappear

First Principal components of HS image

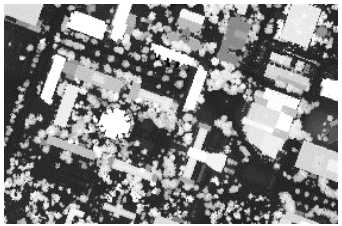

LiDAR data

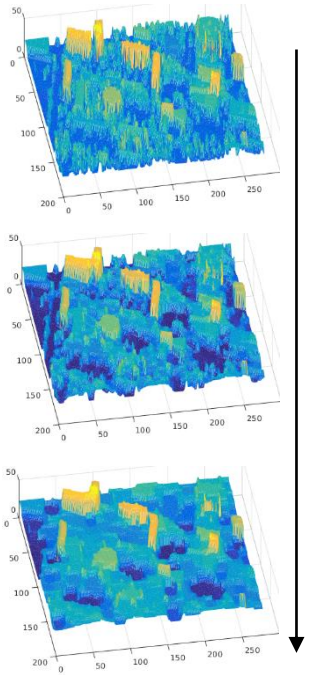

Openings

# Multi-level features

**High-level deep learning features**

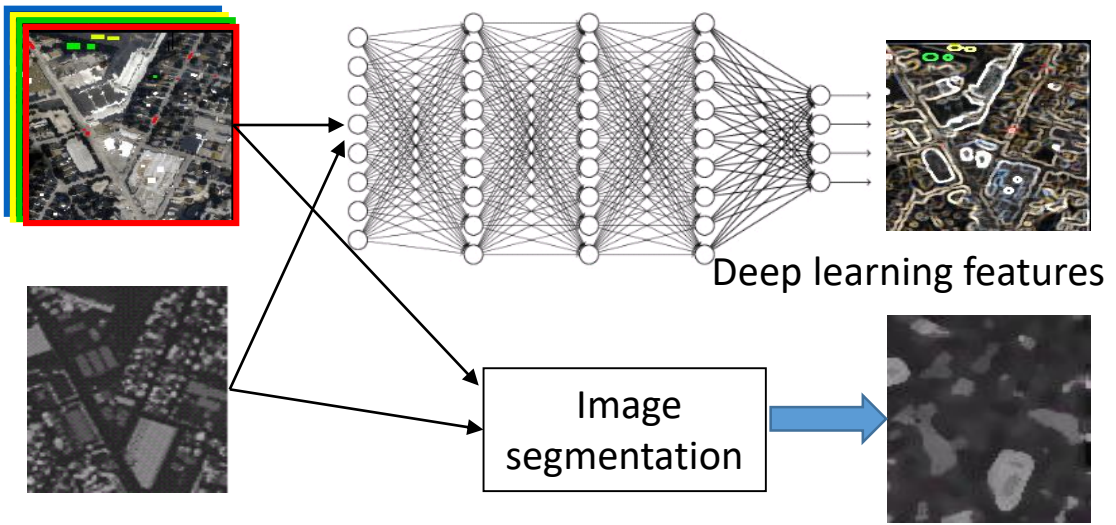


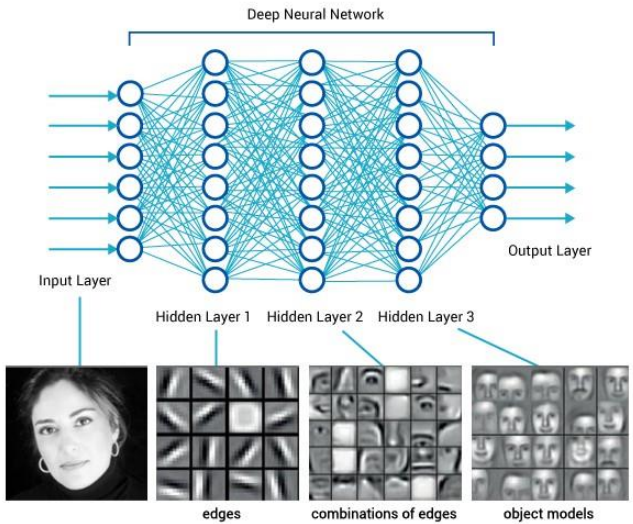

# Multi-level features

**Autoencoders**

Autoencoders are designed to reproduce their input, especially for images

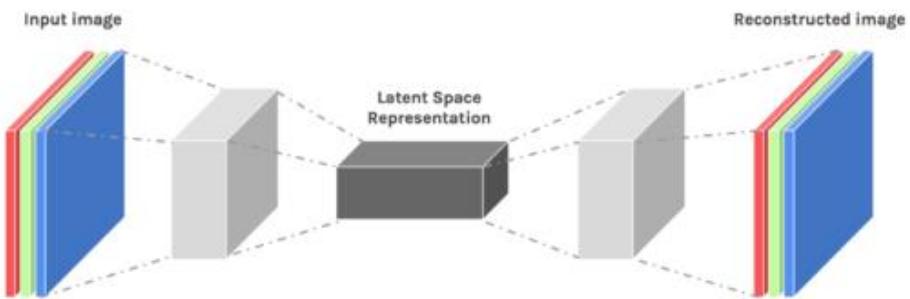


Key point is to reproduce the input from a learned encoding

Compact representation of the input

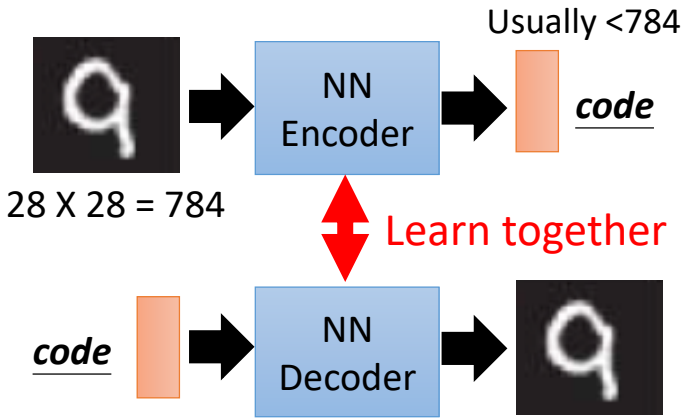


Reconstruct the input

# Multi-level features

**Autoencoders**

- **Encoder**: compress input into a latent-space of usually smaller dimension. h = f(x)
- **Decoder**: reconstruct input from the latent space. r = g(f(x)) with r as close to x as possible

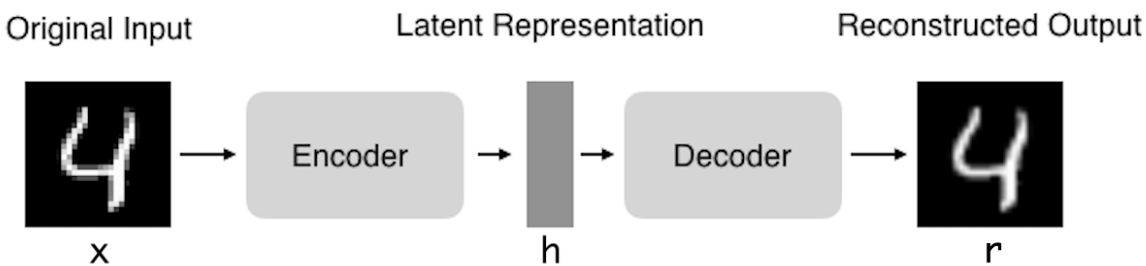


https://towardsdatascience.com/deep-inside-autoencoders-7e41f319999f

# Multi-level features

**PCA**

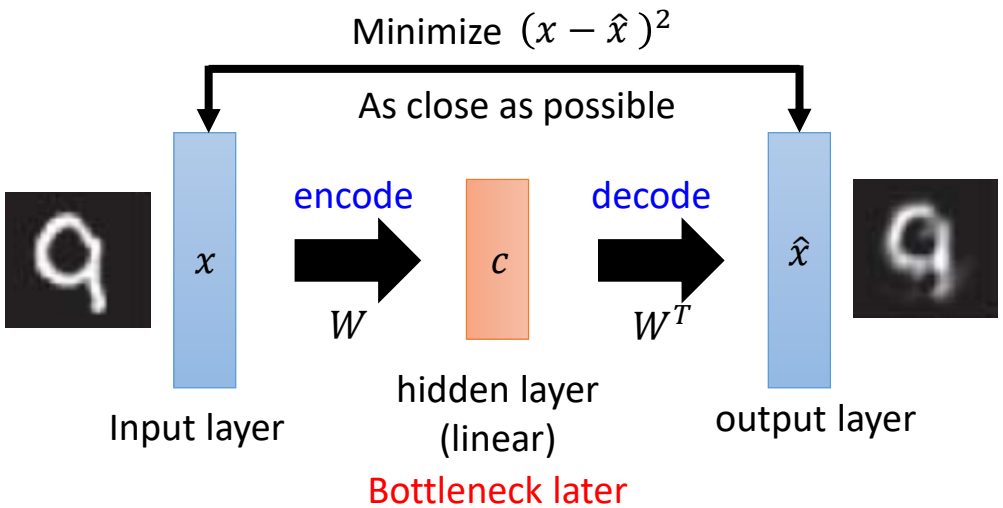


Output of the hidden layer is the code

# Multi-level features

**Autoencoders**

Of course, the auto-encoder can be deep

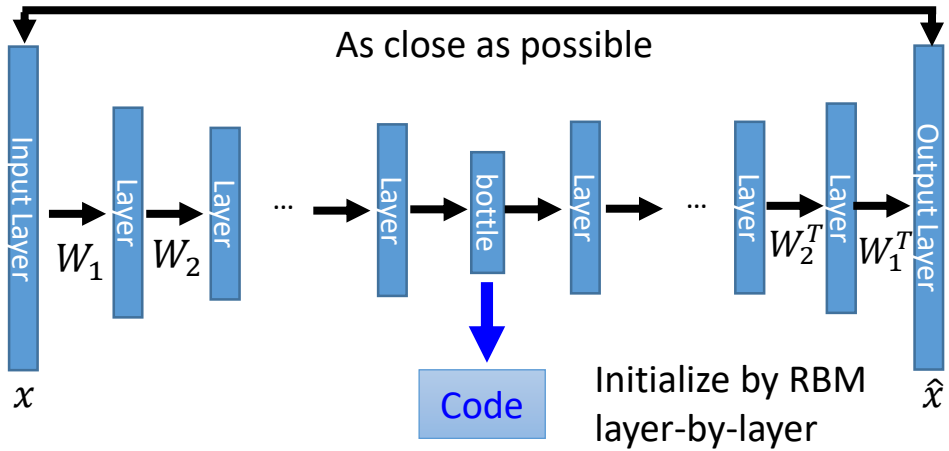


Reference: Hinton, Geoffrey E., and Ruslan R. Salakhutdinov. "Reducing the dimensionality of data with neural networks." *Science* 313.5786 (2006): 504-507

# Multi-level features

**Deep autoencoders**

Original Image

PCA

Deep Auto-encoder

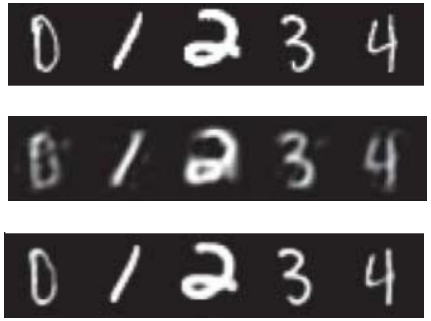

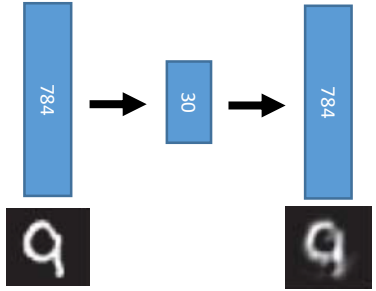


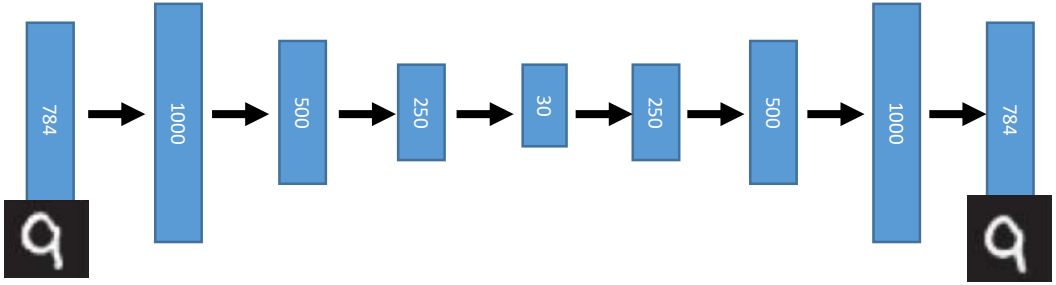

# Multi-level features

**Deep autoencoders**

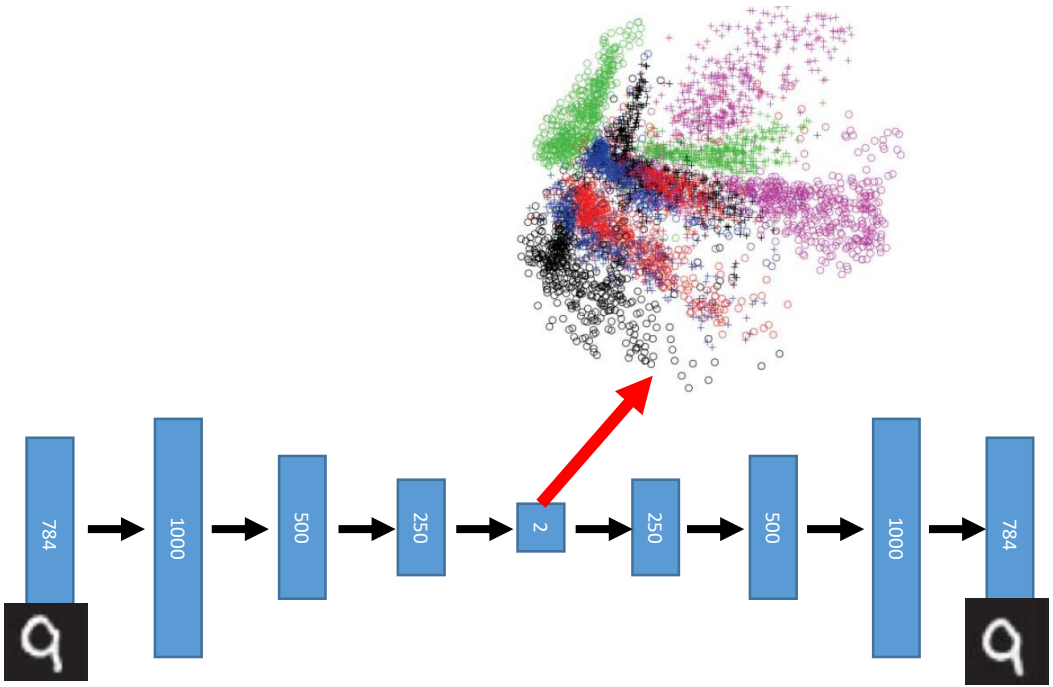


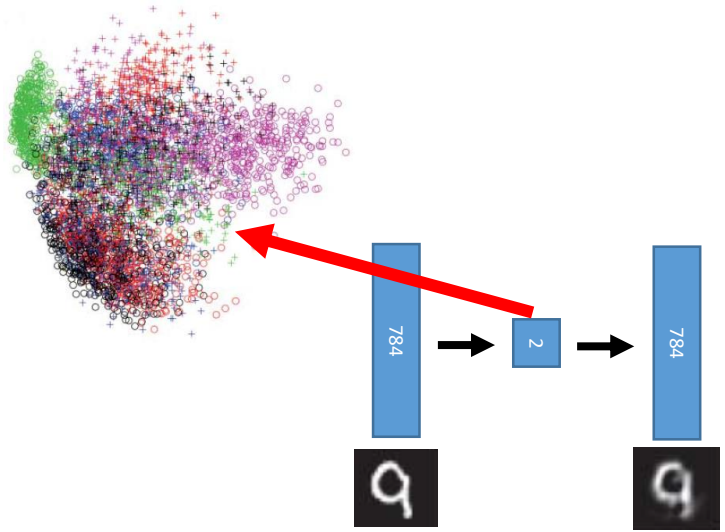

# Multi-level features

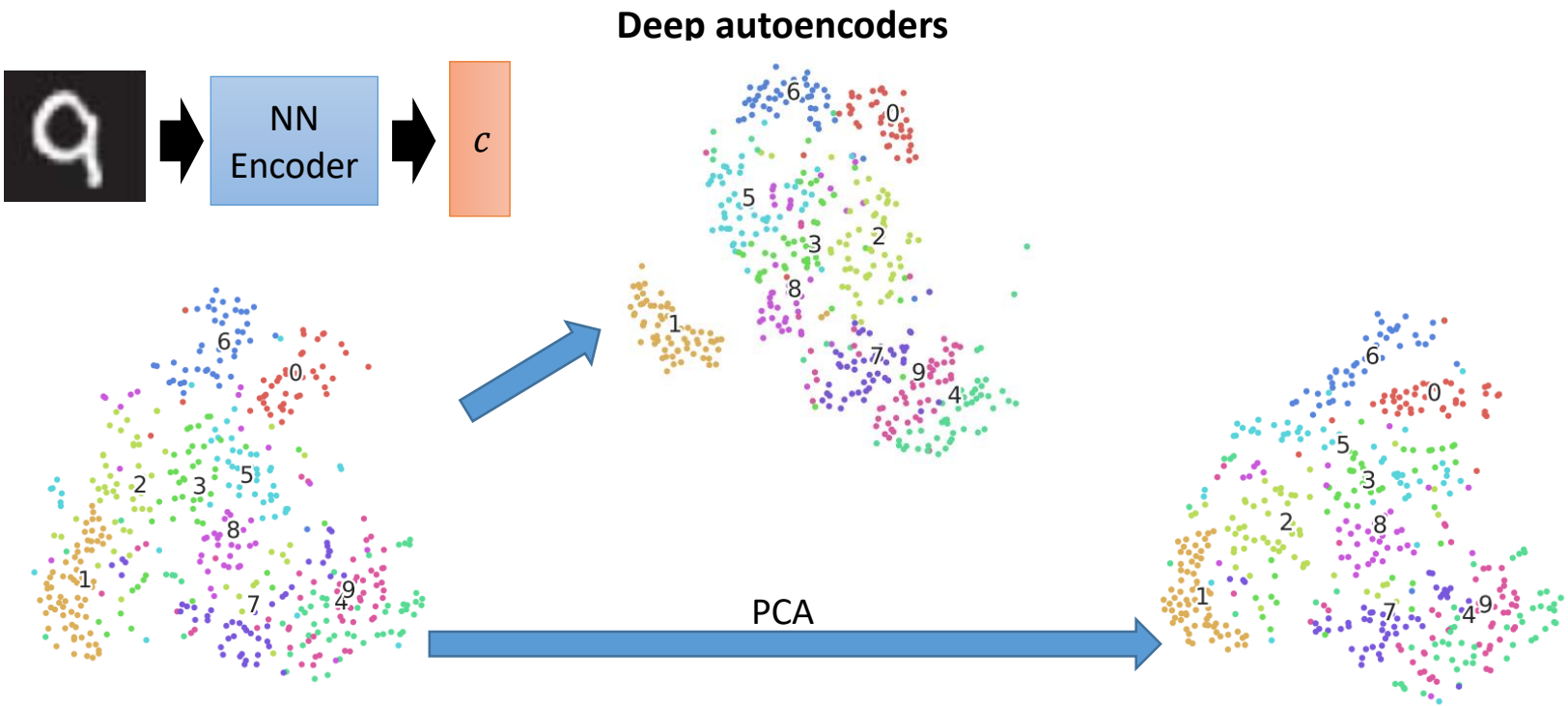

# Multi-level features

**Auto-encoder – Pre-training DNN**

Greedy Layer-wise Pre-training *again*

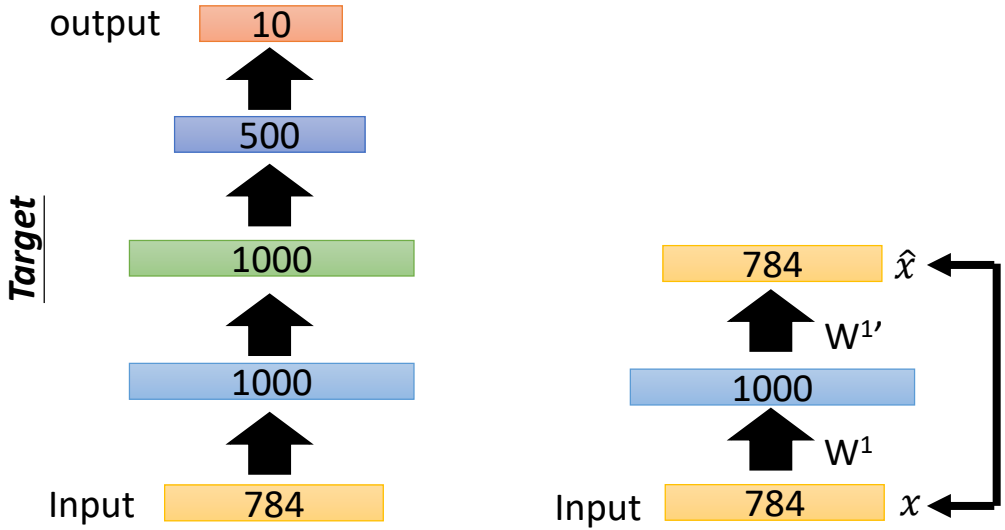

# Multi-level features

**Auto-encoder – Pre-training DNN**

Greedy Layer-wise Pre-training *again*

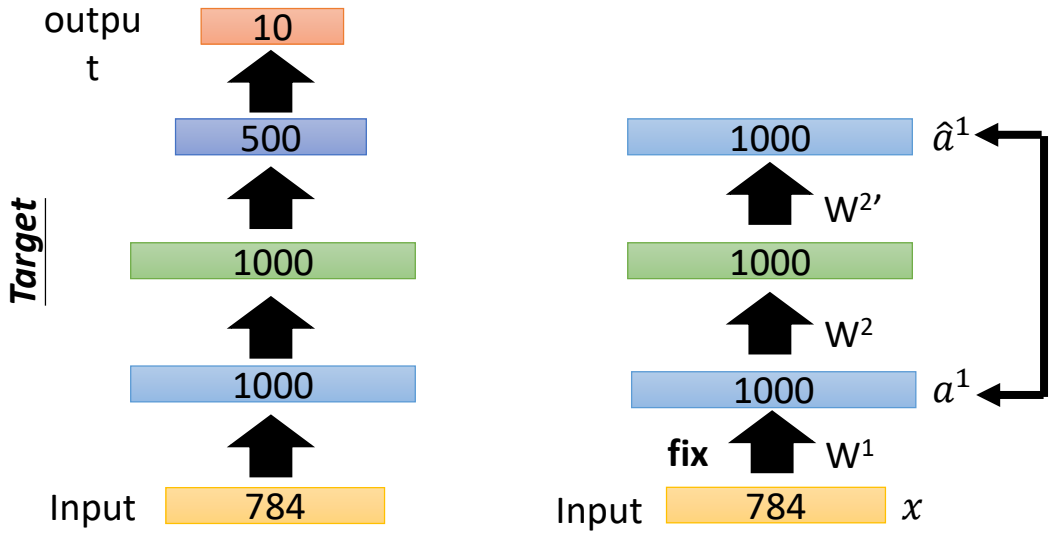

# Multi-level features

**Auto-encoder – Pre-training DNN**

Greedy Layer-wise Pre-training *again*

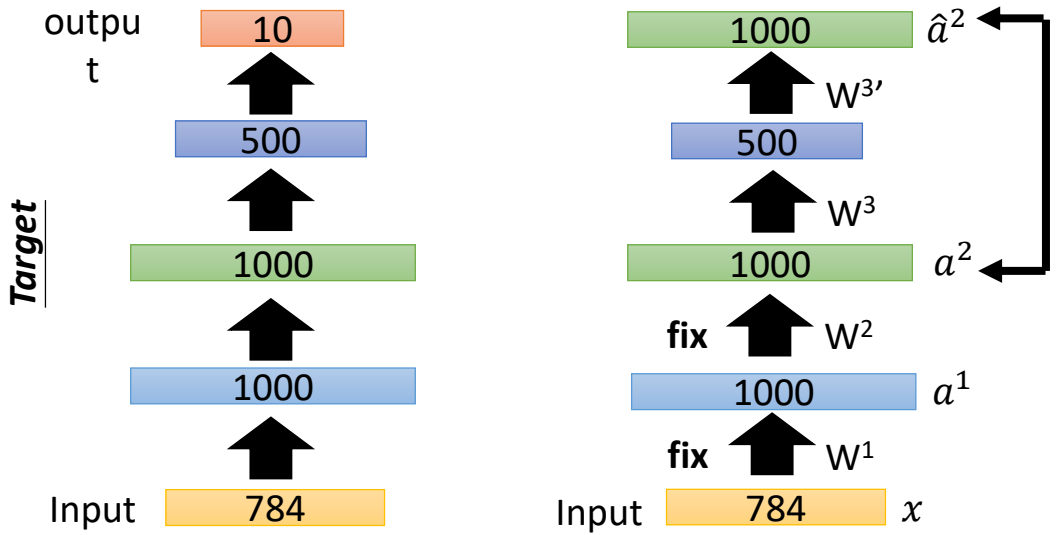

# Multi-level features

**Auto-encoder – Pre-training DNN**

Greedy Layer-wise Pre-training *again*

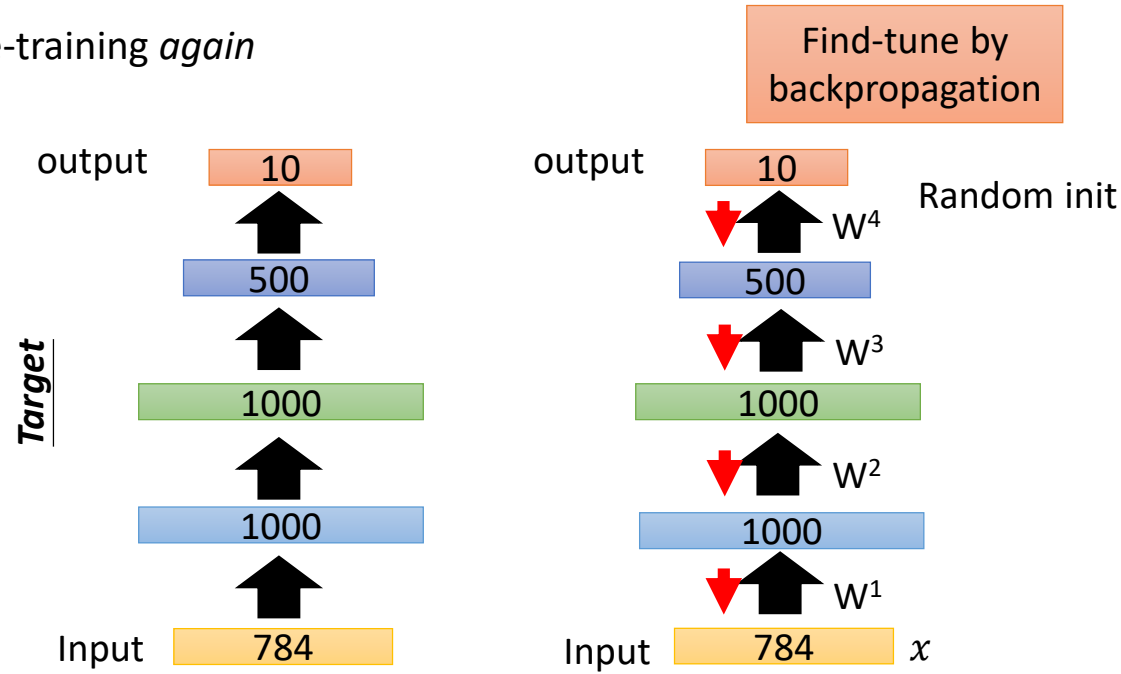

# Methods for data fusion

# Data Fusion frameworks

**Fusion by simply stacking**

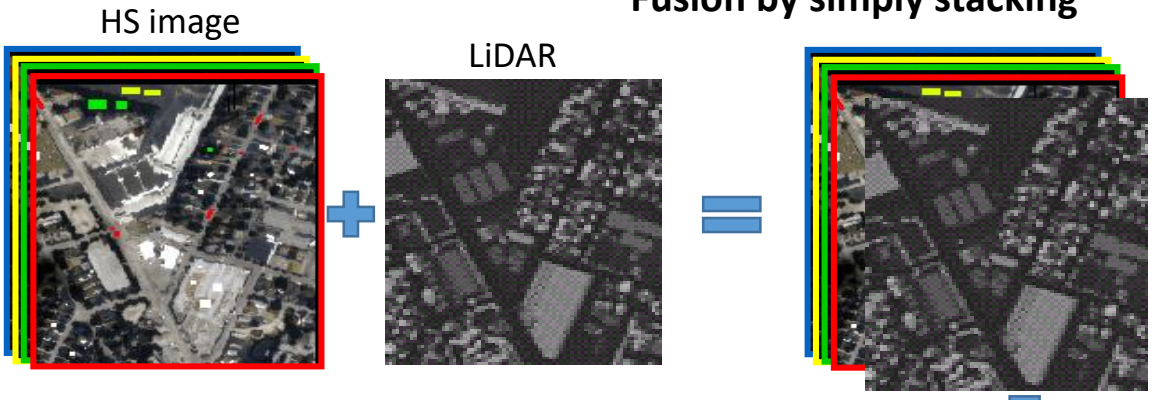


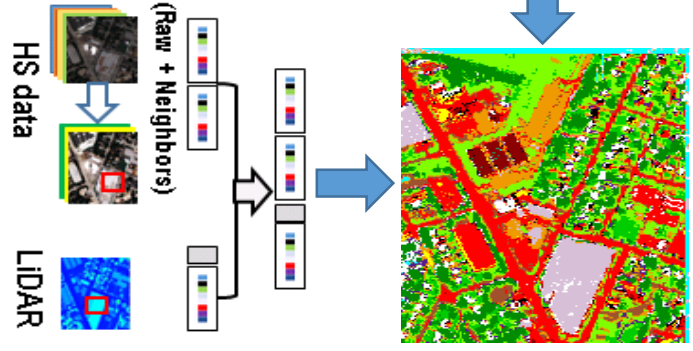


✓Simple and easy

× Increase the dimension

× Complementary information not well exploited

M. Pedergnana, P. Reddy Marpu, et al. (2012), "Classification of Remote Sensing Optical and LiDAR Data Using Extended Attribute Profiles," IEEE Journals on Selected Topics in Signal Processing, 6(7): 856–865.

# Data Fusion frameworks

## Fusion by simply stacking

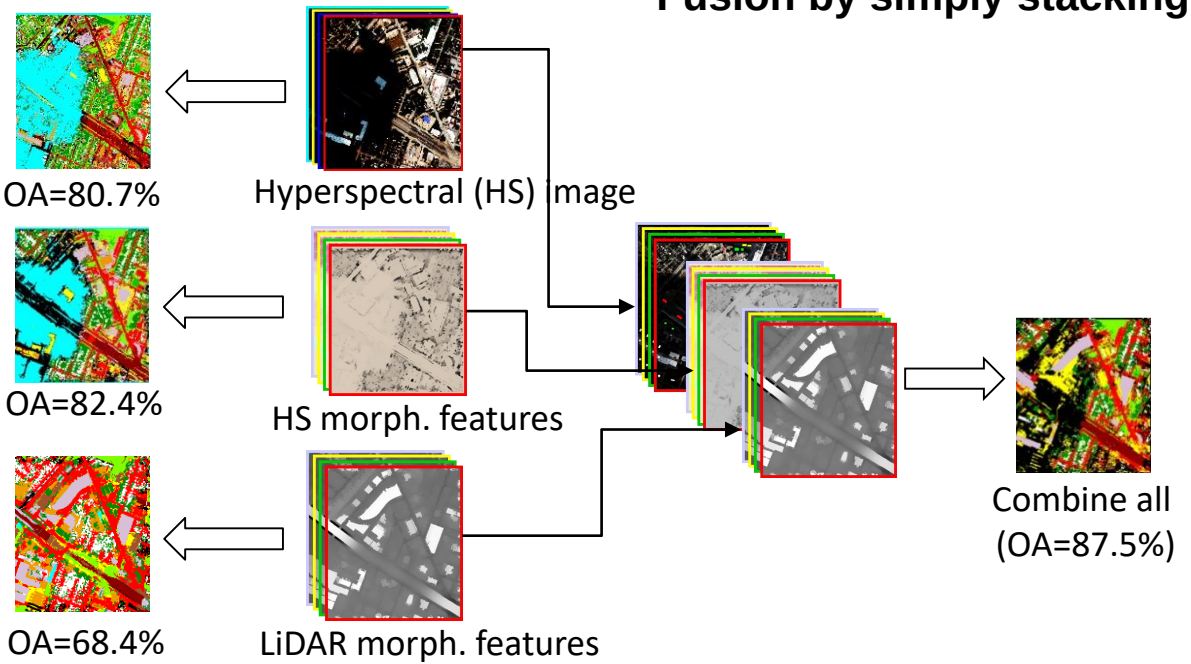


- Single feature source is not sufficient for a reliable classification
- Simply combining all feature sources cannot solve the problems

# Data Fusion frameworks

**Complementary information in the multi-sensor data**

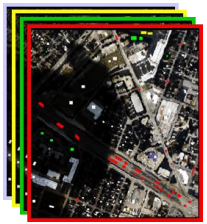

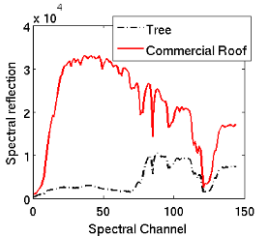


**Hyperspectral (HS) image** provides spectral information to identify the materials

**LiDAR morphological features** discriminate objects with different elevation

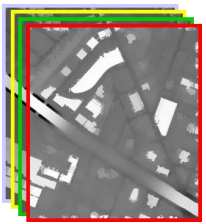

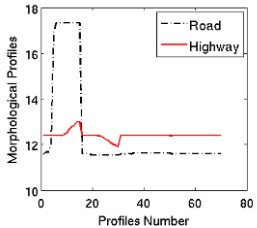

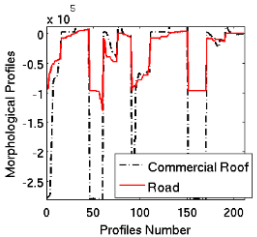


**HS morphological features** discriminate objects with different size/shape

# Data Fusion frameworks

**Graph-based fusion**

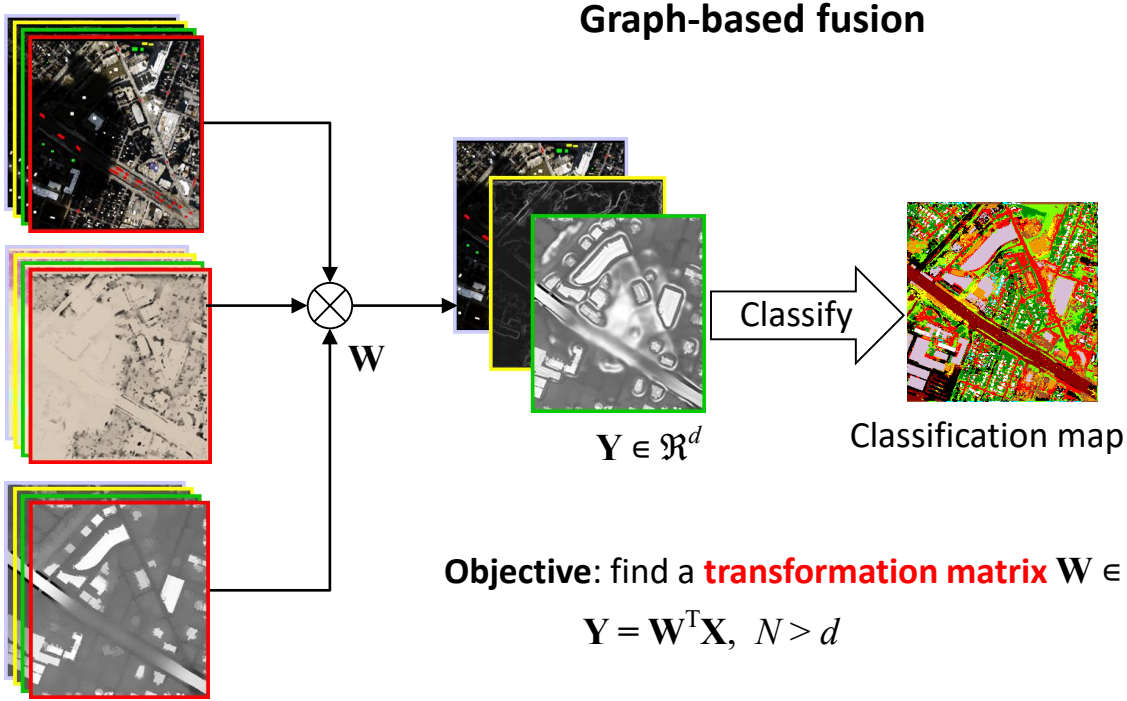


**Reduce** the complexities and redundancy **while exploiting** the complementary information

**Objective**: find a **transformation matrix** $\mathbf{W} \in \Re^{N \times d}$

$$\mathbf{Y} = \mathbf{W}^{\mathrm{T}}\mathbf{X}, \quad N > d$$

$\mathbf{X}^{Sta} = [\mathbf{X}^{Spe}; \mathbf{X}^{Spa}; \mathbf{X}^{Ele}] \in \Re^N$

# Data Fusion frameworks

## Graph-based fusion

**Graph G=(V,E)**

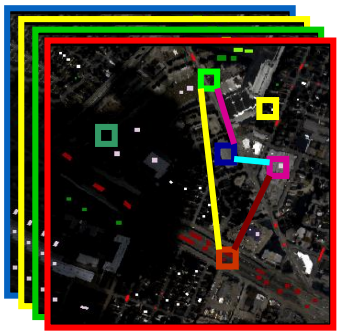

The node **V** means data points $[\mathbf{x}_1, \mathbf{x}_2, \ldots, \mathbf{x}_n]$

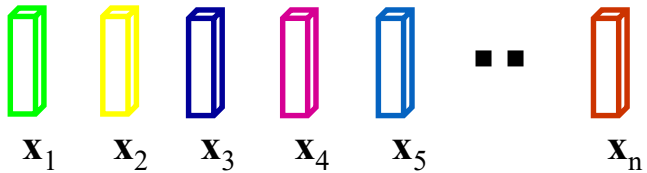


The edge **E** denotes 'connection' and 'similarity' between nodes

C. Debes, et al. (2014), "Hyperspectral and LiDAR Data Fusion: Outcome of the 2013 GRSS Data Fusion Contest," IEEE Journal of Selected Topics in Applied Earth Observations and Remote Sensing, 7(6): 2405-2418.

# Data Fusion frameworks

## Graph-based fusion

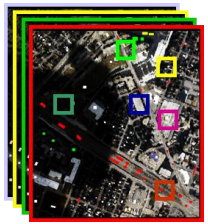

Hyperspectral image

$$
\begin{array}{c|cccccc}
 & x_1^{Spe} & x_2^{Spe} & x_3^{Spe} & x_4^{Spe} & x_5^{Spe} & x_6^{Spe} \\
\hline
x_1^{Spe} & 0 & 1 & 0 & 1 & 1 & 0 \\
x_2^{Spe} & 1 & 0 & 0 & 1 & 0 & 1 \\
x_3^{Spe} & 0 & 0 & 0 & 1 & 1 & 1 \\
x_4^{Spe} & 1 & 1 & 1 & 0 & 0 & 0 \\
x_5^{Spe} & 1 & 0 & 1 & 0 & 0 & 1 \\
x_6^{Spe} & 0 & 1 & 1 & 0 & 1 & 0
\end{array}
$$

$$\mathbf{G}^{Spe}=(\mathbf{V}^{Spe},\ \mathbf{E}^{Spe})$$

$E_{3,4}^{Spe}=1$ means $x_3^{Spe}$ and $x_4^{Spe}$ have similar spectral reflection

...

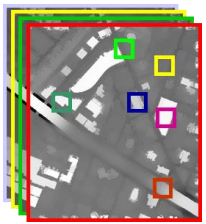

LiDAR features

$$
\begin{array}{c|cccccc}
 & x_1^{Spe} & x_2^{Spe} & x_3^{Spe} & x_4^{Spe} & x_5^{Spe} & x_6^{Spe} \\
\hline
x_1^{Spe} & 0 & 1 & 0 & 0 & 1 & 1 \\
x_2^{Spe} & 1 & 0 & 0 & 1 & 0 & 1 \\
x_3^{Spe} & 0 & 0 & 0 & 1 & 1 & 1 \\
x_4^{Spe} & 0 & 1 & 1 & 0 & 1 & 0 \\
x_5^{Spe} & 1 & 0 & 1 & 1 & 0 & 0 \\
x_6^{Spe} & 1 & 1 & 1 & 0 & 0 & 0
\end{array}
$$

$$\mathbf{G}^{Ele}=(\mathbf{V}^{Ele},\ \mathbf{E}^{Ele})$$

$E_{3,4}^{Ele}=1$ means $x_3^{Ele}$ and $x_4^{Ele}$ have similar elevation

# Data Fusion frameworks

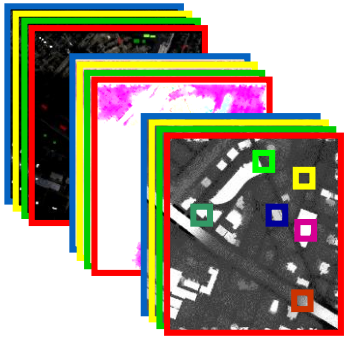

Stacking all morphological profiles

## Graph-based fusion

Construct the fusion graph **G*=(V*,E*)**:

$$\mathbf{V}^*=[\mathbf{V}^{Spe};\mathbf{V}^{Spa};\mathbf{V}^{Ele}],\quad \mathbf{E}^*=\mathbf{E}^{Spe}\odot\mathbf{E}^{Spa}\odot\mathbf{E}^{Ele},$$

$$\mathbf{X}^{Sta}=[\mathbf{X}^{Spe};\mathbf{X}^{Spa};\mathbf{X}^{Ele}]$$

$E_{i,j}$*=1 means $\mathbf{x}_i^{Sta}$ and $\mathbf{x}_j^{Sta}$ have similar characteristics on all terms of spectral, spatial and elevation.

$$\begin{array}{c|cccccc} & x_1^{Sta} & x_2^{Sta} & x_3^{Sta} & x_4^{Sta} & x_5^{Sta} & x_6^{Sta} \\ \hline x_1^{Sta} & 0 & 0 & 0 & 0 & 1 & 0 \\ x_2^{Sta} & 0 & 0 & 0 & 1 & 0 & 1 \\ x_3^{Sta} & 0 & 0 & 0 & 1 & 0 & 1 \\ x_4^{Sta} & 0 & 1 & 1 & 0 & 0 & 0 \\ x_5^{Sta} & 1 & 0 & 0 & 0 & 0 & 0 \\ x_6^{Sta} & 0 & 1 & 1 & 0 & 0 & 0 \end{array} = \begin{bmatrix} 0&1&0&1&1&0\\1&0&0&1&0&1\\0&0&0&1&1&1\\1&1&1&0&0&0\\1&0&1&0&0&1\\0&1&1&0&1&0 \end{bmatrix} \odot \begin{bmatrix} 0&0&1&1&1&0\\0&0&0&1&1&1\\1&0&0&1&0&1\\1&1&1&0&0&0\\1&1&0&0&0&1\\0&1&1&0&1&0 \end{bmatrix} \odot \begin{bmatrix} 0&1&0&0&1&1\\1&0&0&1&0&1\\0&0&0&1&1&1\\0&1&1&0&1&0\\1&0&1&1&0&0\\1&1&1&0&0&0 \end{bmatrix}$$

$$G^{Spe}=(V^{Spe},E^{Spe}) \qquad G^{Spa}=(V^{Spa},E^{Spa}) \qquad G^{Ele}=(V^{Ele},E^{Ele})$$

**G*=(V*,E*)**

# Data Fusion frameworks

## Graph-based fusion

**Solve** $\underset{\mathbf{W} \in \Re^{3D \times d}}{\arg\min} \sum_{i,j=1}^{n} ||\mathbf{W}^T x_i^{Sta} - \mathbf{W}^T x_j^{Sta}||^2 E_{i,j}^*$

$$\Downarrow$$

$$\mathbf{W}^T \mathbf{X}^{Sta} = \mathbf{Y}$$

**The proposed method won the "Best Paper" award of 2013 IEEE GRSS Data Fusion Contest**

**Codes:** https://telin.ugent.be/~wliao/Research.html

$\mathbf{W}^T$ *

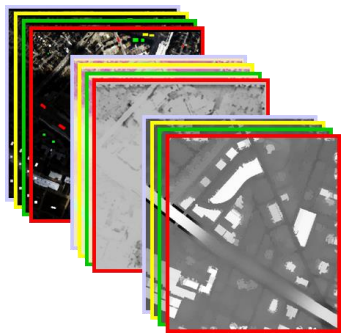

=

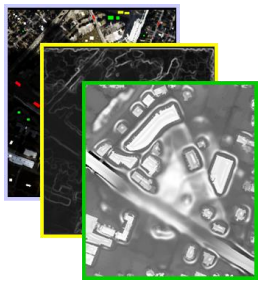

$\mathbf{X}^{Sta} = [\mathbf{X}^{Spe}; \mathbf{X}^{Spa}; \mathbf{X}^{Ele}] \in \Re^{3D}$

$\mathbf{Y} \in \Re^{d}$

W. Liao, et al. (2015), "Generalized Graph-Based Fusion of Hyperspectral and LiDAR Data Using Morphological Features," IEEE Geoscience and Remote Sensing Letters, 12(3): 552-556.

# Data Fusion frameworks

**Deep learning fusion**

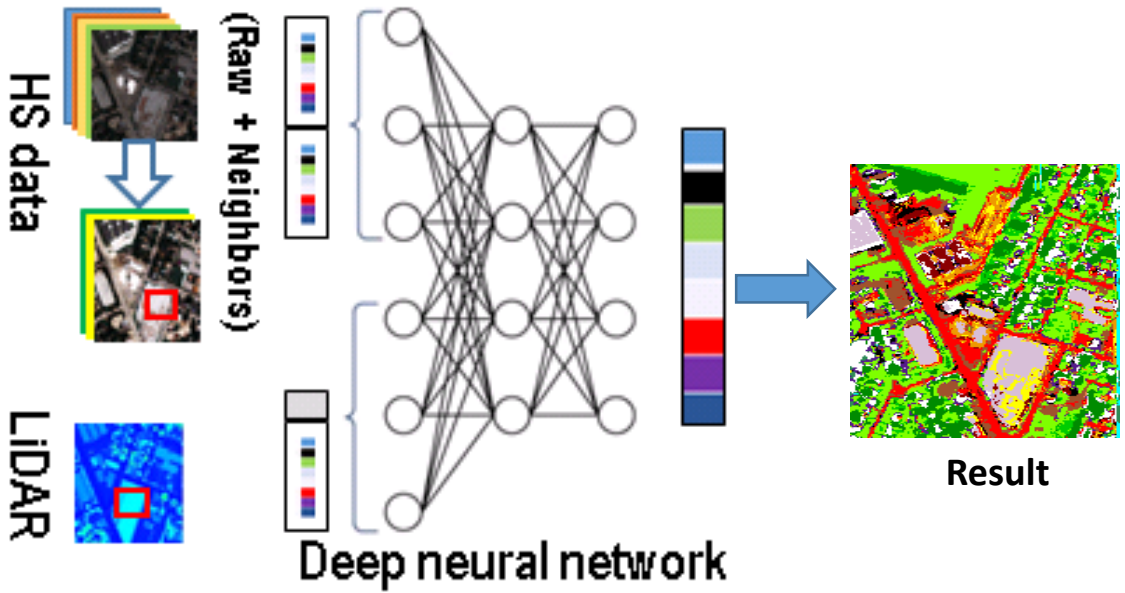

# Experimental comparisons

# Experimental data

**False color image of original hyperspectral image with 144 bands**

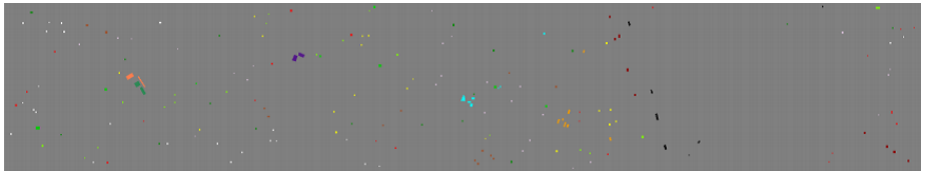

**Training samples**

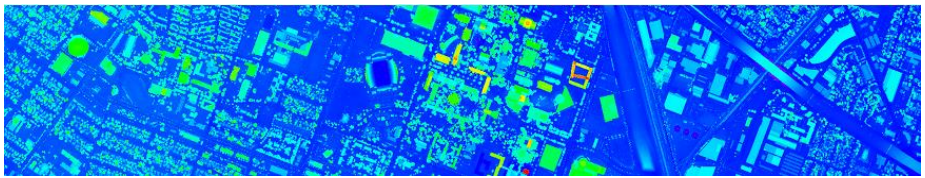

**LiDAR image**

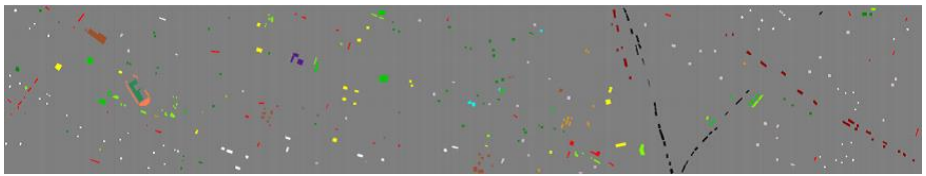

**Test samples**

2.5 m spatial resolution

15 classes

# Experimental data

HS image (OA=77.96%)

HS image (OA=84.02%)

HS image (OA=77.36%)

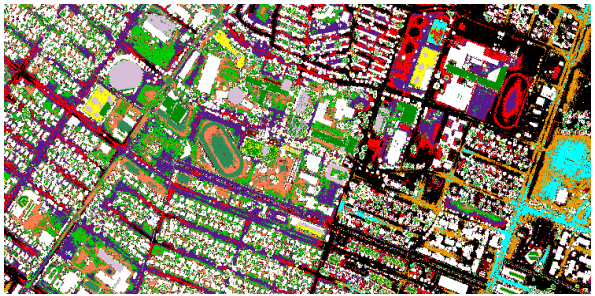

LiDAR image (OA=31.34%)

LiDAR image (OA=75.43%)

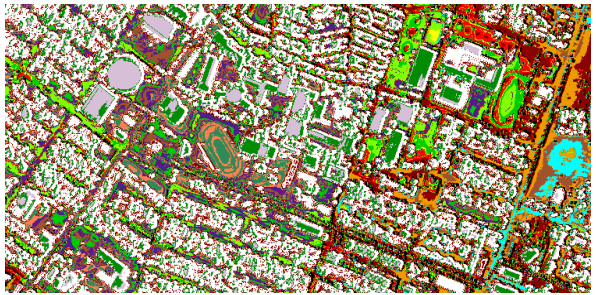

LiDAR image (OA=42.86%)

**Raw**

**Morphological profiles**

**Deep Learning**

# Experimental data

Stacking raw data (OA=79.6%)

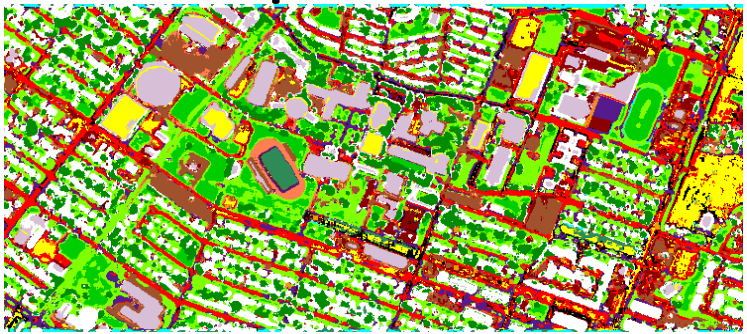

Stacking neighborhood features(OA=81.5%)

Graph fusion MPs (OA=89.9%)

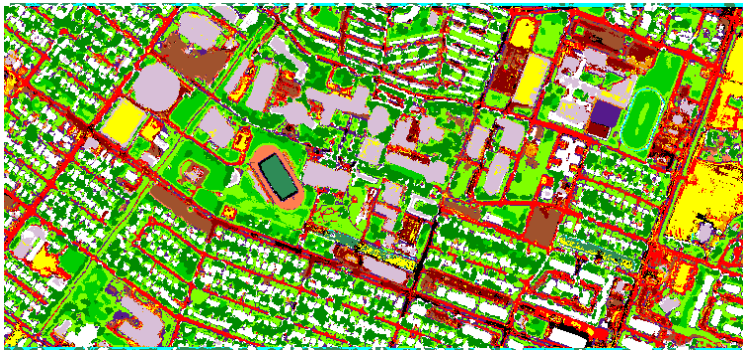

Deep learning fusion (OA=81.9%)

# Fusion results

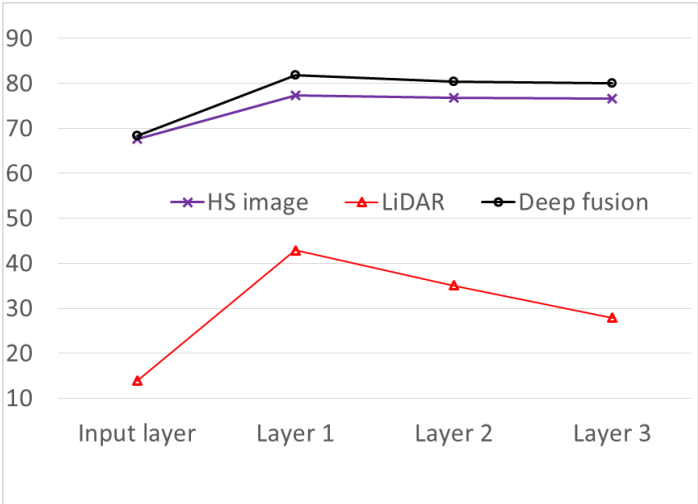


- ✓ Multi-level features were exploited: morphological features outperform low-level and high-level deep learning features
- ✓ Graph-based fusion outperform than fusion by stacking and deep fusion

# Fractional Gabor Network for Multi-source classification

# Motivation

Multi-source， Multi-feature fusion: Octave Convolutional layers

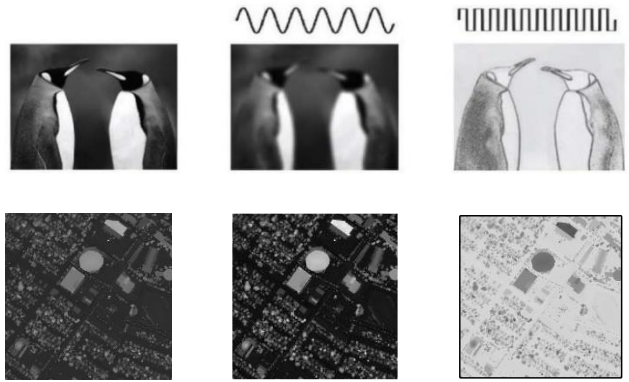

***Redundant Information in Single Source***

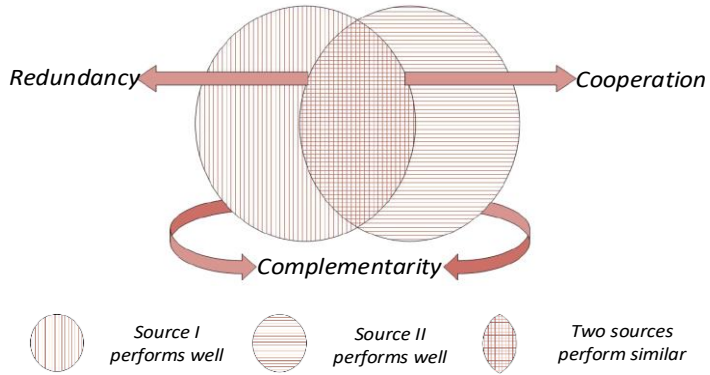


***Multi-source Fusion***

***Reduce redundancy, improve cooperation***

# Motivation

Spatial-Spectral → Spatial-Spectral-Textural-Frequency:

Fractional Gabor Convolutional Layers

Complex spatial information

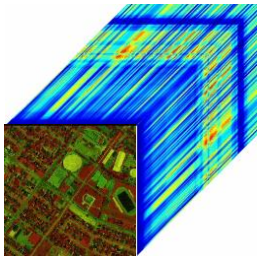

***Limited Training Set*** → ***Multi-domain Features***

# Method

- ***Multi-Source Data***
- ***Multi-source Feature***
- ***Limited Training Set***

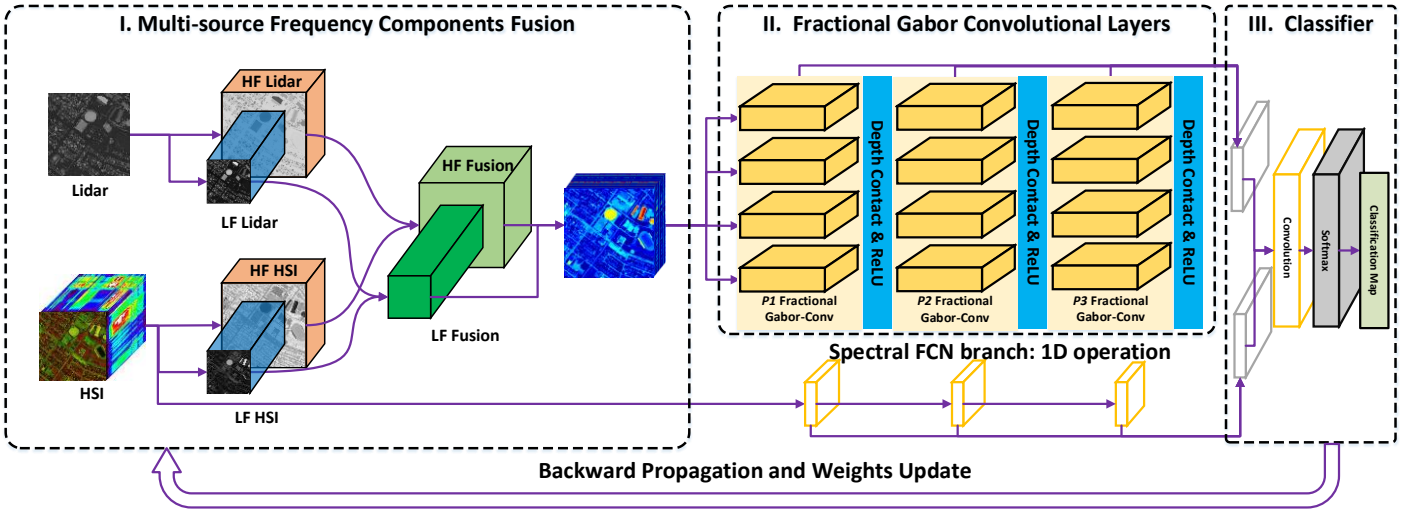


[2021 TGRS] Zhao, X., Tao, R., Li, W., Philips, W. & Liao, W. (2021). Fractional Gabor Convolutional Network for Multi-source Remote Sensing Data Classification[J]. IEEE Transactions on Geoscience and Remote Sensing, 2021, DOI:10.1109/TGRS.2021.3065507. Github code link: https://github.com/xudongzhao461/FGCN

# Experimental data

COMPARISON OF THE CLASSIFICATION ACCURACY (%) USING THE HOUSTON DATA.

| No. | Class(Train/Test) | Performance | | | | | | | |
|---|---|---|---|---|---|---|---|---|---|
| | | SVM | RF | OTVCA | CRNN | TB-CNN | CCNN | CNNMRF | FGCN |
| 1 | Healthy grass (100/1053) | 95.44 | 95.80 | 98.94 | 92.50 | 86.51 | 95.38 | 92.15 | 98.72 |
| 2 | Stressed grass (100/1064) | 97.85 | 94.53 | 96.89 | 99.15 | 97.27 | 94.82 | 91.78 | 98.30 |
| 3 | Synthetic grass (100/505) | 100.00 | 99.15 | 100.00 | 100.00 | 100.00 | 100.00 | 99.71 | 98.87 |
| 4 | Trees (100/1056) | 94.61 | 96.46 | 99.59 | 97.44 | 94.22 | 97.70 | 98.23 | 98.54 |
| 5 | Soil (100/1056) | 99.11 | 96.53 | 99.76 | 99.81 | 99.72 | 99.76 | 99.27 | 99.91 |
| 6 | Water (100/143) | 96.92 | 93.52 | 99.39 | 99.30 | 98.60 | 100.00 | 99.38 | 100.00 |
| 7 | Residential (100/1072) | 92.11 | 86.07 | 96.88 | 88.81 | 87.69 | 88.91 | 95.45 | 98.15 |
| 8 | Commercial (100/1036) | 93.81 | 89.31 | 99.58 | 88.13 | 91.07 | 95.32 | 98.19 | 97.68 |
| 9 | Road (100/1059) | 88.34 | 78.71 | 97.73 | 85.84 | 88.20 | 81.92 | 91.42 | 97.27 |
| 10 | Highway (100/1036) | 94.13 | 85.36 | 96.31 | 96.91 | 80.41 | 88.18 | 94.87 | 98.87 |
| 11 | Railway (100/1054) | 95.79 | 79.67 | 94.56 | 94.40 | 89.85 | 85.04 | 92.03 | 97.58 |
| 12 | Parking lot 1 (100/1041) | 88.48 | 84.78 | 97.53 | 76.66 | 88.28 | 82.96 | 99.65 | 98.18 |
| 13 | Parking lot 2 (100/285) | 81.66 | 57.24 | 84.97 | 97.89 | 98.25 | 78.21 | 86.35 | 98.97 |
| 14 | Tennis court (100/247) | 99.53 | 95.28 | 97.94 | 100.00 | 100.00 | 98.38 | 90.85 | 100.00 |
| 15 | Running track (100/473) | 99.70 | 99.10 | 99.40 | 100.00 | 100.00 | 98.21 | 98.06 | 100.00 |
| OA | | 94.34 | 88.63 | 97.51 | 93.01 | 91.60 | 91.67 | 95.15 | **98.50** |
| Kappa | | 93.88 | 87.71 | 97.31 | 92.42 | 90.88 | 91.00 | 94.76 | **98.38** |
| AA | | 94.50 | 88.77 | 97.30 | 94.46 | 93.34 | 92.32 | 95.16 | **98.74** |

# Experimental data

**Dataset 3： Trento, 6 classes**

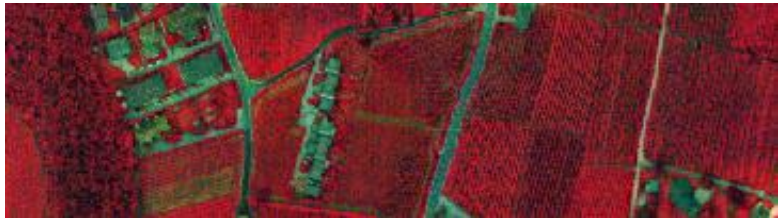

HSI

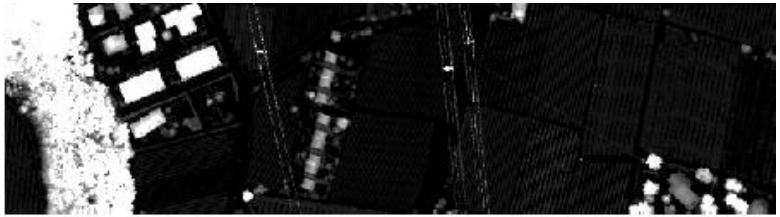

LiDAR

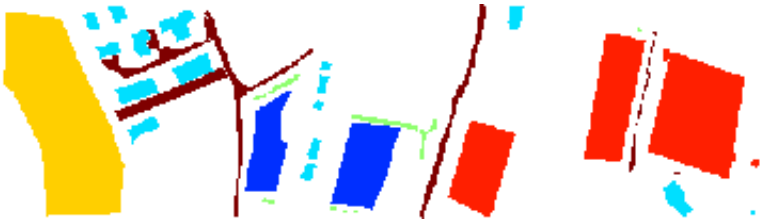

Ground truth

- Trento  Data was acquired over a rural area in the south of the city of Trento, Italy.
- The data are composed of 600*166 pixels covering 6 classes with a spatial resolution of 1m.
- The HSI data comprise 63 spectral bands covering the range from 0.42 to 0.99 μm .

# Experimental data

COMPARISON OF THE CLASSIFICATION ACCURACY (%) USING THE TRENTO DATA.

| No. | Class(Train/Test) | Performance | | | | | | | |
|---|---|---|---|---|---|---|---|---|---|
| | | SVM | RF | OTVCA | CRNN | TB-CNN | CCNN | CNNMRF | FGCN |
| 1 | Apple trees (50/3905) | 89.49 | 67.42 | 99.34 | 99.23 | 98.74 | 92.09 | 99.21 | 99.32 |
| 2 | Buildings (50/2778) | 76.47 | 81.47 | 93.50 | 90.25 | 91.87 | 90.08 | 88.82 | 96.88 |
| 3 | Ground (50/374) | 97.70 | 67.72 | 98.54 | 100.00 | 99.37 | 94.78 | 76.13 | 96.04 |
| 4 | Woods (50/8969) | 93.63 | 97.46 | 99.94 | 99.68 | 99.93 | 99.38 | 100.00 | 100.00 |
| 5 | Vineyard (50/10317) | 73.53 | 90.66 | 99.14 | 99.81 | 99.88 | 98.77 | 99.34 | 99.68 |
| 6 | Roads (50/3525) | 73.91 | 81.40 | 92.09 | 92.19 | 95.09 | 91.21 | 85.48 | 98.78 |
| OA | | 82.44 | 86.44 | 98.12 | 97.98 | 98.46 | 96.37 | 96.60 | **99.32** |
| Kappa | | 77.03 | 82.09 | 97.49 | 97.30 | 97.95 | 95.15 | 95.47 | **99.09** |
| AA | | 84.12 | 81.02 | 97.09 | 96.86 | 97.48 | 94.38 | 91.50 | **98.45** |

# Experimental data

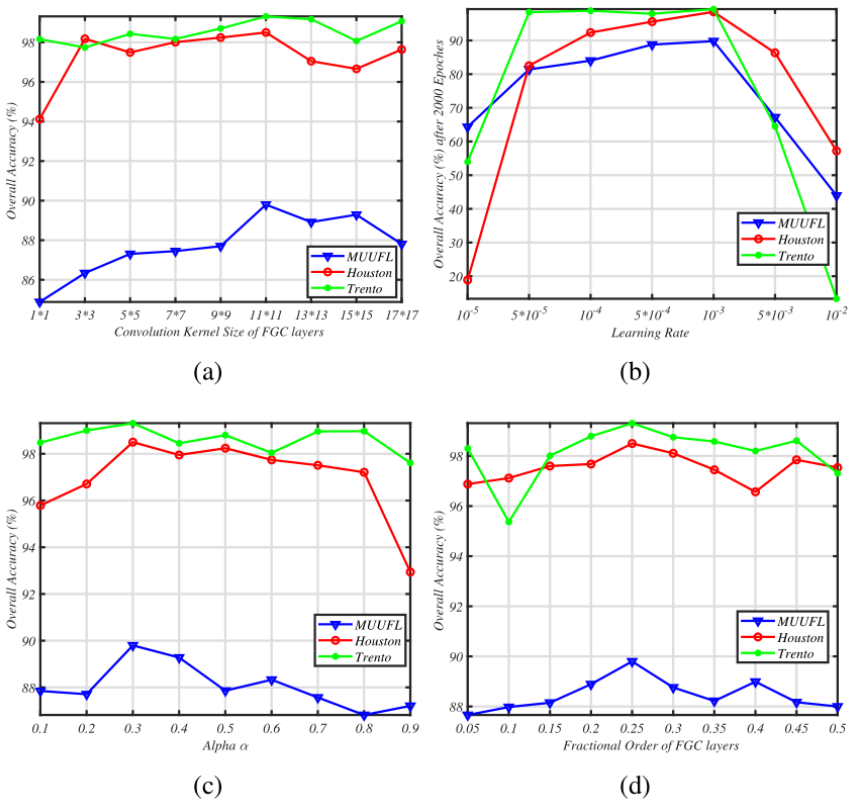


**Parameter Tunning**

Classification performance of different convolution kernel size, learning rate, low frequency rate, fractional order using FGCN .

# Experimental data

ABLATION ANALYSIS OF THE PROPOSED FGCN IN TERMS OF OA (%) AND KAPPA (%) ON THE THREE DATASETS.

| Spectral | Spatial | Spatial-Spectral | LiDAR | Fractional Gabor | Methods | MUUFL | | Houston | | Trento | |
|---|---|---|---|---|---|---|---|---|---|---|---|
| | | | | | | OA | Kappa | OA | Kappa | OA | Kappa |
| √ | × | × | × | × | SpecFCN | 67.49 | 58.99 | 54.25 | 51.14 | 61.42 | 50.91 |
| × | √ | × | × | × | SpatFCN | 76.49 | 69.88 | 90.58 | 89.80 | 97.05 | 96.05 |
| √ | √ | √ | × | × | SSFCN | 80.87 | 75.34 | 92.11 | 91.46 | 96.88 | 95.82 |
| √ | √ | √ | √ | × | Octave-FFSCN | 85.46 | 81.11 | 96.73 | 96.46 | 98.55 | 98.06 |
| √ | √ | √ | √ | √ | FGCN | 89.21 | 85.91 | 98.50 | 98.38 | 99.18 | 98.91 |

**Ablation Analysis:**

- Octave convolution layers can greatly improve the classification accuracy.
- The difference between Octave-SSFCN and FGCN shows that fractional Gabor convolutional layers add diversity, discrimination, and robustness.
- Spectral-Spatial feature contribute more than single kind.

# Experimental data

## Robustness Analysis

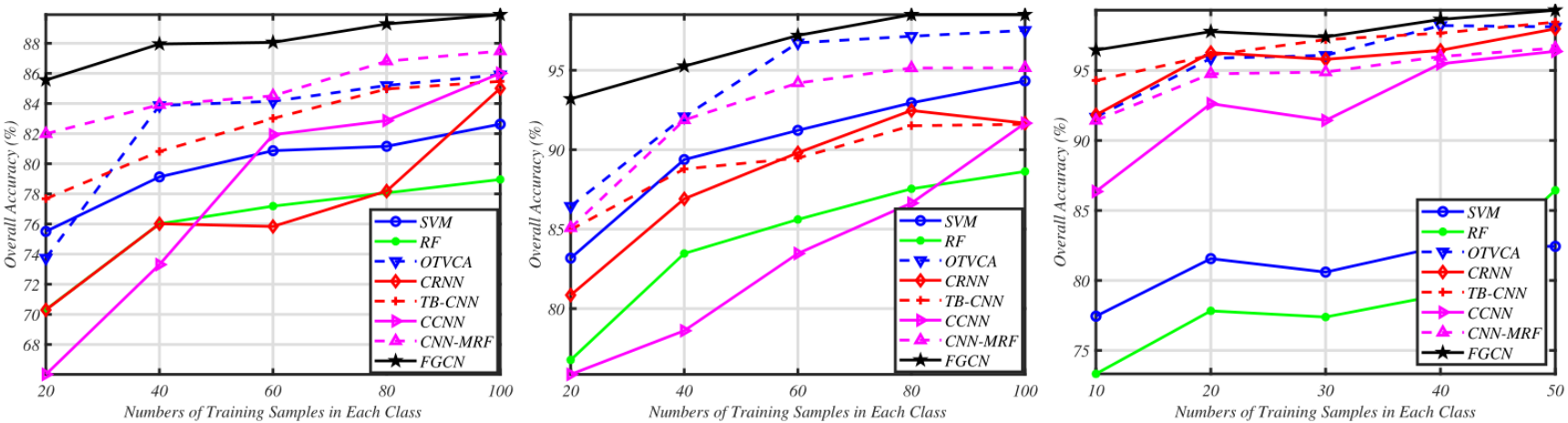


**Robustness to size of labeled samples**, the proposed method consistently outperforms other methods using limited training samples.

# Experimental data

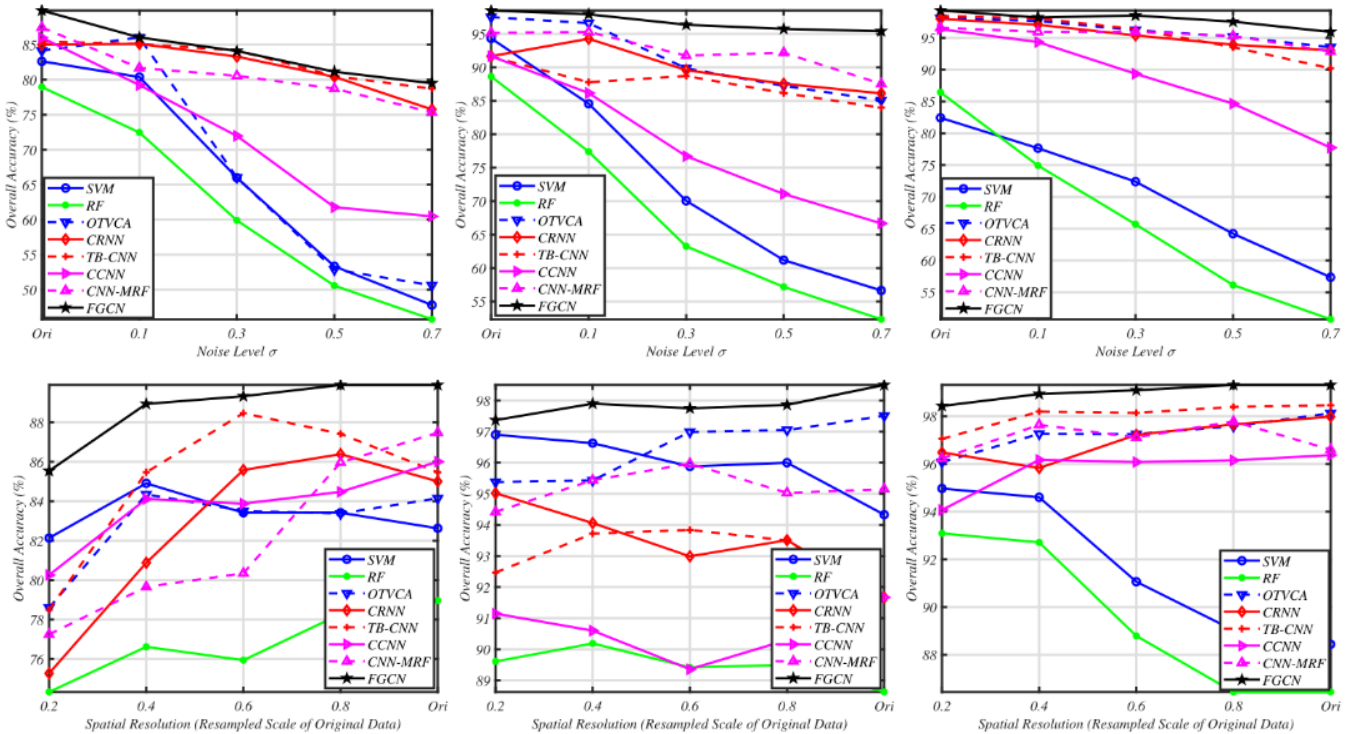


**Robustness under noisy condition, low spatial resolution condition.**

# Fusion of Hyperspectral and LiDAR Data for Classification of Cloud-Shadow Mixed Remote Sensed Scene

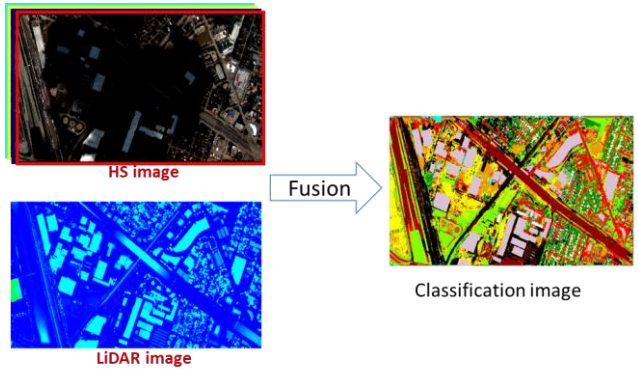


R. Luo, W. Liao, H. Zhang, L. Zhang, P. Scheunders, Y. Pi, W. Philips, "Fusion of Hyperspectral and LiDAR Data for Classification of Cloud-Shadow Mixed Remote Sensed Scene", IEEE JSTARS, vol. 10, no. 8, pp. 3768 - 3781, 2017.

# Classification under shadow

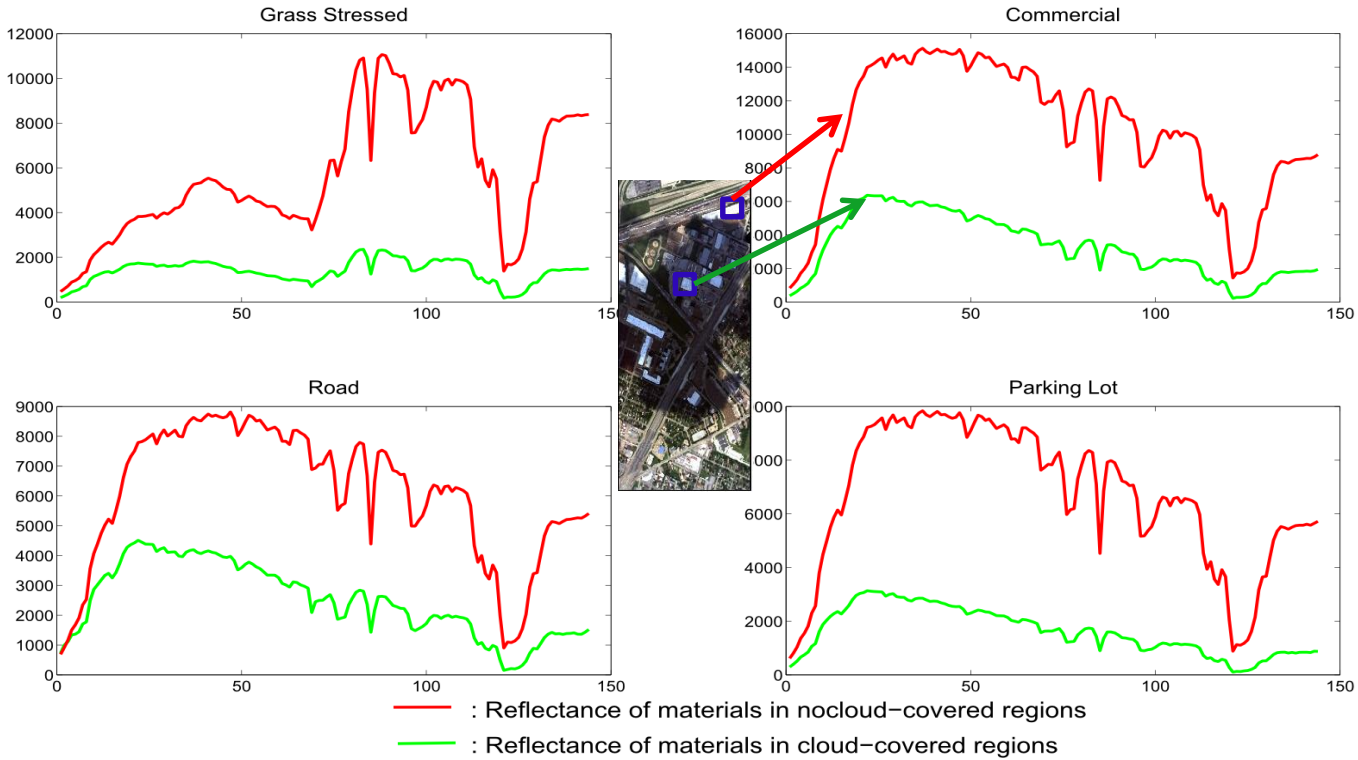

# Classification under shadow

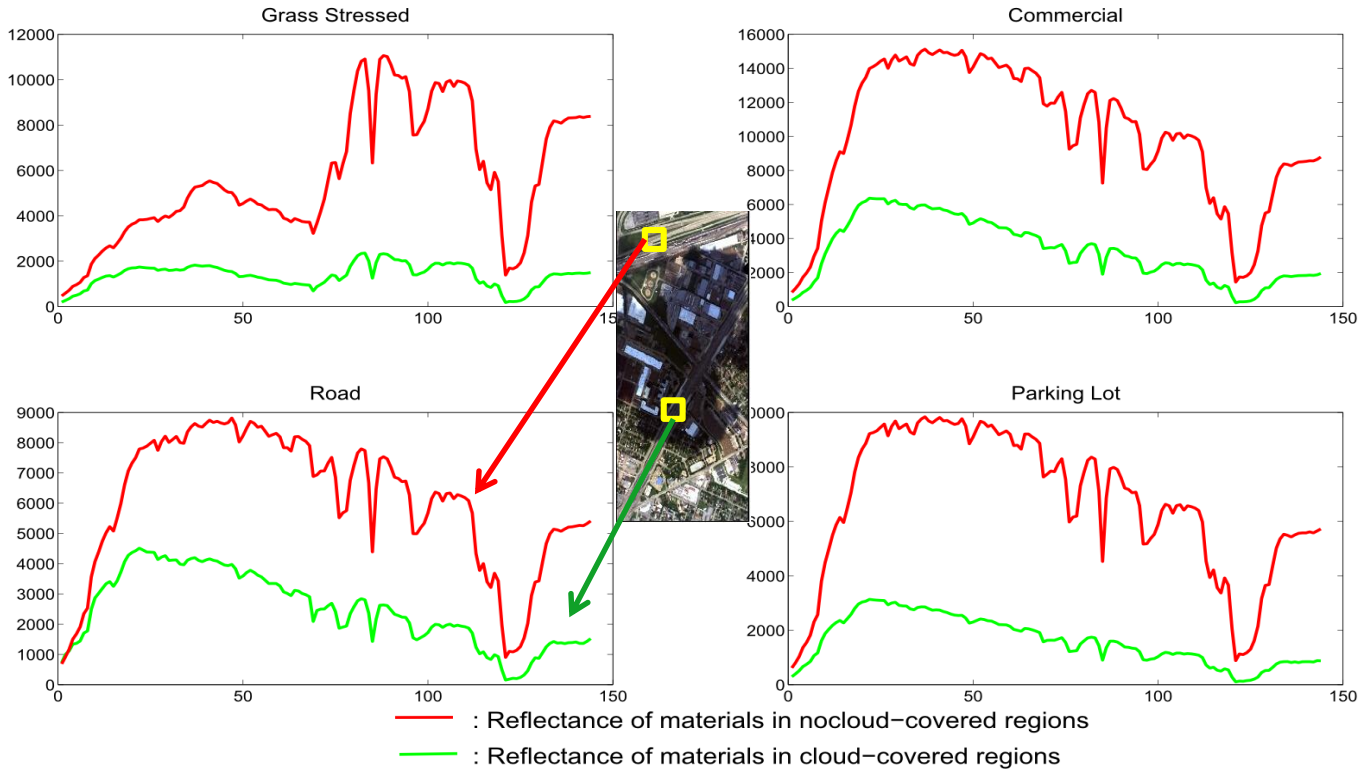

# Classification under shadow

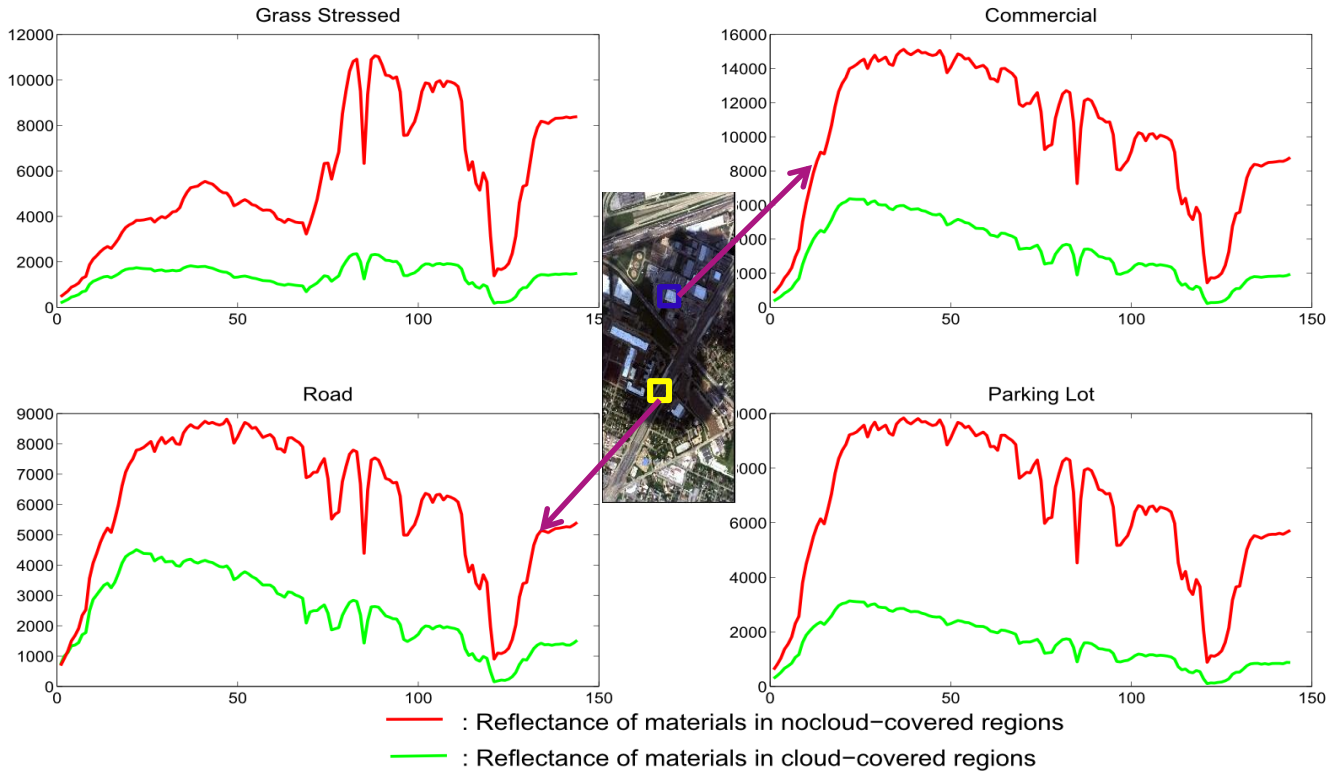

# Classification under shadow

**Proposed fusion method**

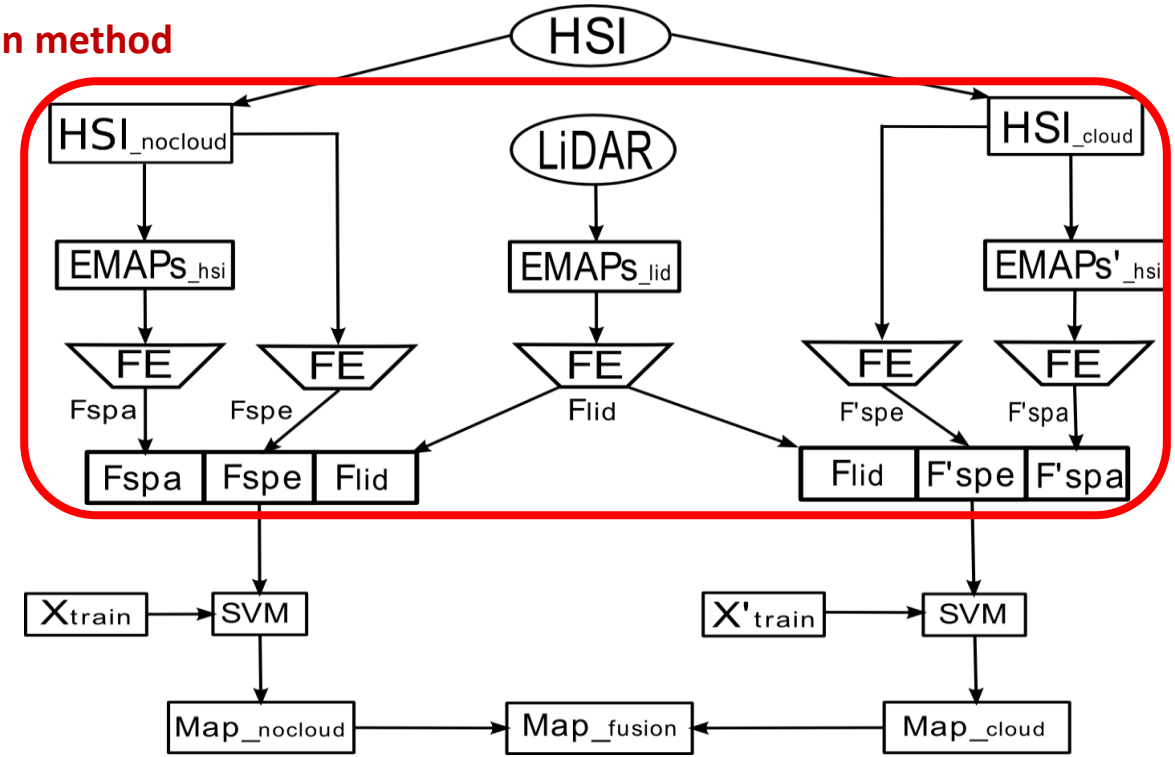

# Classification under shadow

Area attribute profiles(>5000)

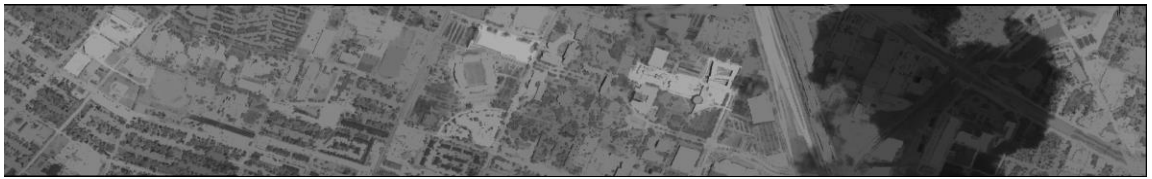

Binarization

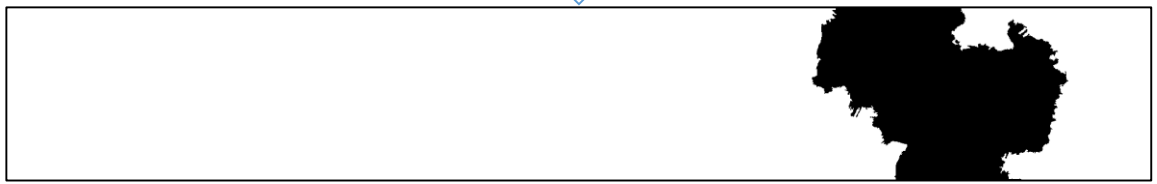

**Cloud mask extraction**

# Classification under shadow

**Proposed fusion method**

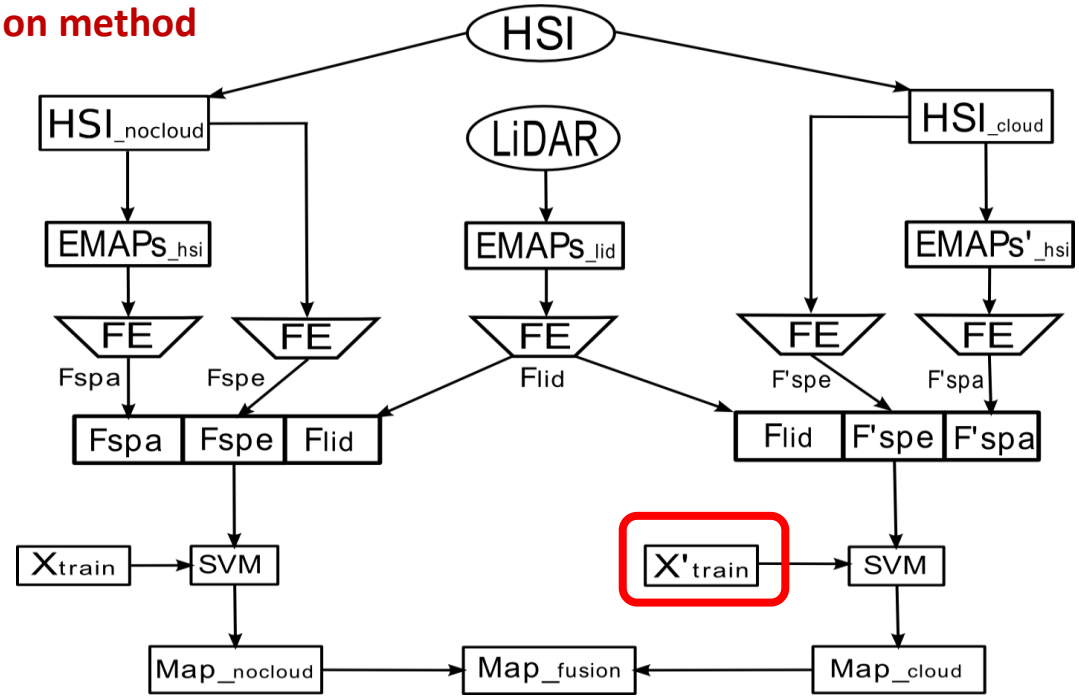

# Classification under shadow

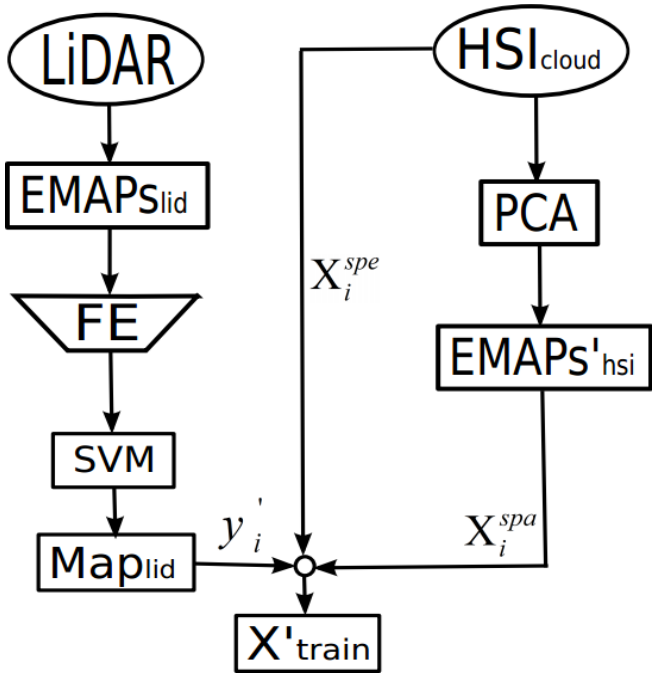


**Proposed: Co-training samples selection**

# Classification under shadow

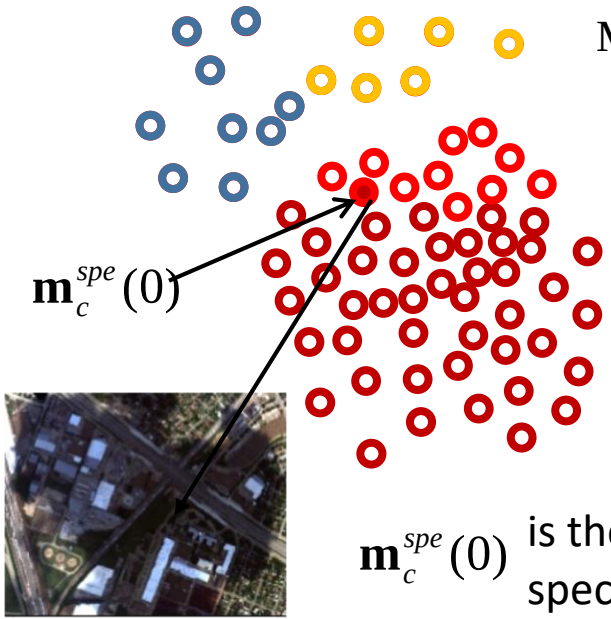


$\mathrm{Map}_{lid}\,(y_i^{'} = c)$

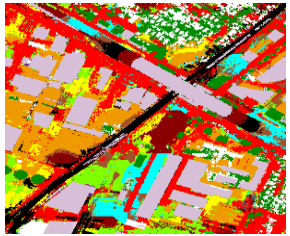

**These samples are misclassified**

$\mathbf{m}_c^{spe}(0)$ is the center of class ***c*** in spectral space

The following samples (under cloud shadow) are classified into the same class $\boldsymbol{c}(y_i^{'} = c)$ based on single LiDAR data.

# Classification under shadow

Select the k-nearest neighbors of the center as training samples under shadow

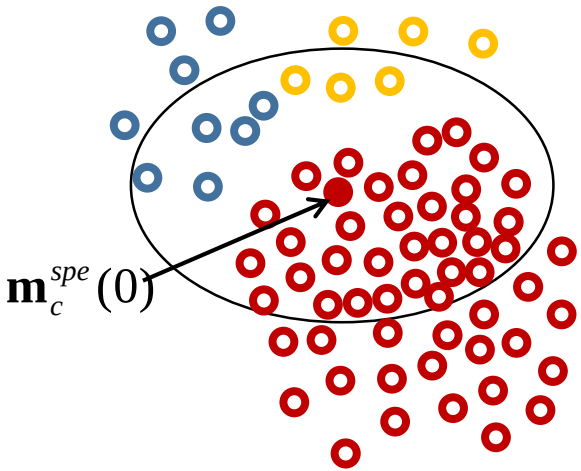

# Classification under shadow

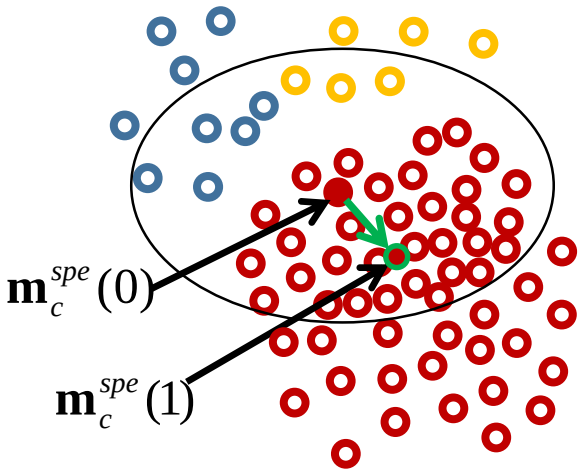


$\mathbf{m}_c^{spe}(1)$ is the center of class ***c***
based on the set $kNN(\mathbf{m}_c^{spe}(0))$

# Classification under shadow

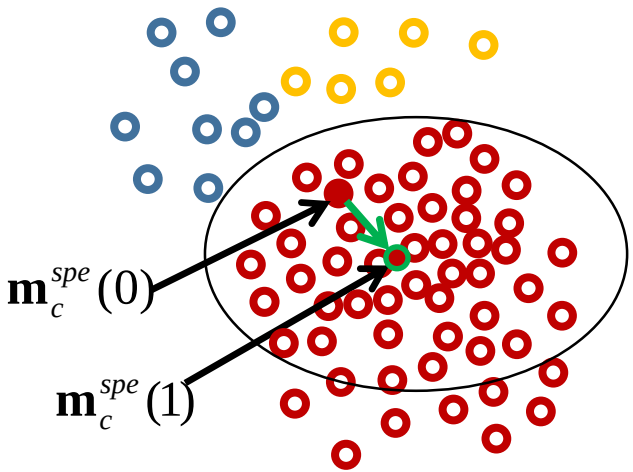


Find the KNN of the new center of spectral features

Find the KNN of the new center of spatial features

$$\mathrm{X}_{train}^{c} = \{\mathrm{x}_i^{Sta} : \mathrm{x}_1^{spe} \in kNN(\mathbf{m}_c^{spe}(1)), \mathrm{x}_1^{spa} \in kNN(\mathbf{m}_c^{spa}(1))\}$$

# Classification under shadow

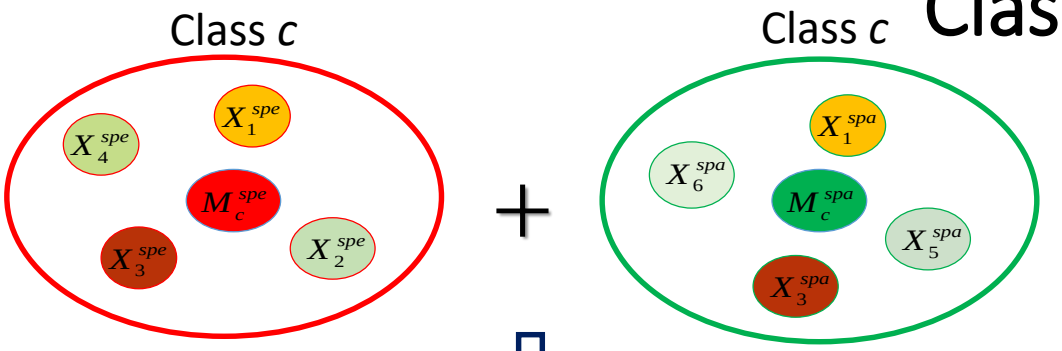


*k*-nearest neighbors in spectral feature space

*k*-nearest neighbors in spatial feature space

$$\mathrm{X}_{train}^{c} = \{\mathrm{x}_1^{Sta}; \mathrm{x}_3^{Sta}\}$$

$$\begin{cases} \mathbf{x}_i^{Sta} = \{\mathbf{x}_i^{spe}; \mathbf{x}_i^{spa}\}, y_i^{'} = c \\ \mathrm{X}_{train}^{c} = \{\mathrm{x}_i^{Sta} : \mathrm{x}_1^{spe} \in kNN(\mathbf{m}_c^{spe}), \mathrm{x}_1^{spa} \in kNN(\mathbf{m}_c^{spa})\} \end{cases}$$

# Classification under shadow

False color image

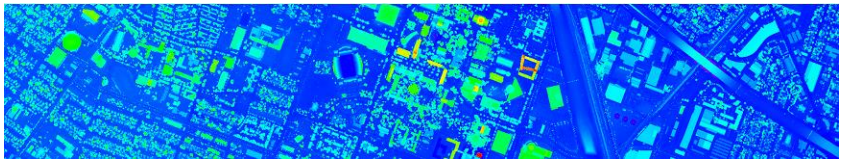

LiDAR image

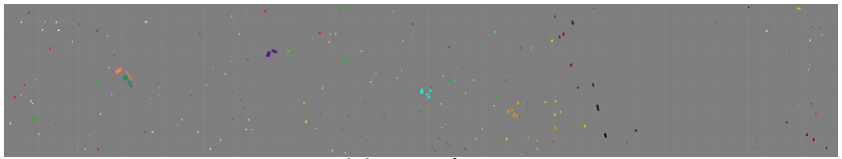

Training samples

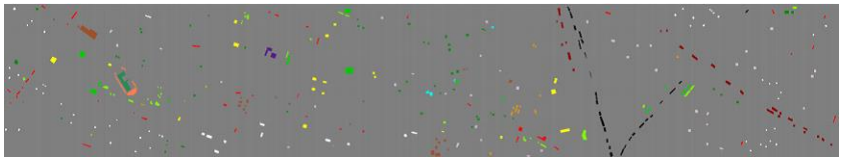

Test samples

Size:
$349 \times 1905$

Bands:
144

Classes:
15

Spatial resolution:
2.5 m/pixel

**Experimental data**

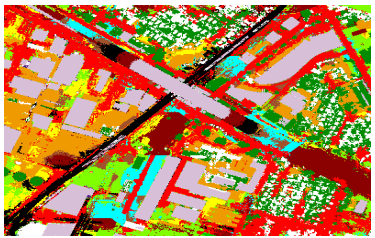

# Classification under shadow

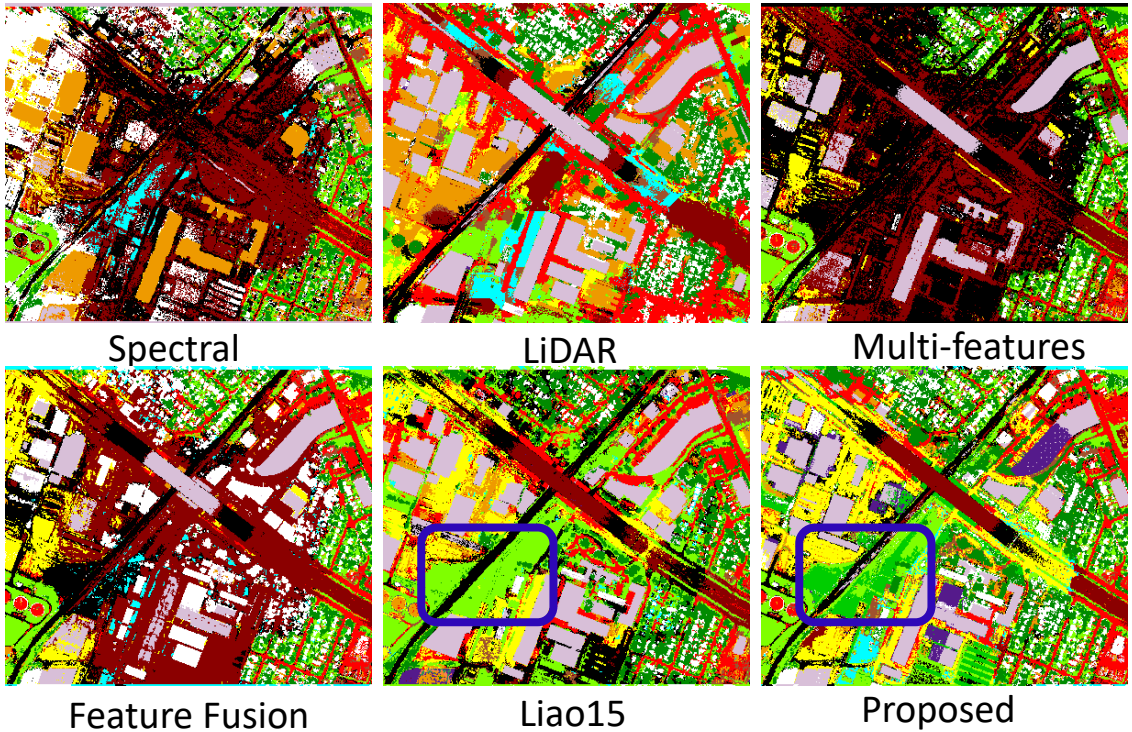


**Classification maps for cloud-covered regions**

# Classification under shadow

| Features | $\text{Raw}_{hsi}$ | $Fspe$ | $Fspa$ | $Flid$ | $FEstacked$ | $Ffusion$ | $Fggf$ | Proposed |
|---|---|---|---|---|---|---|---|---|
| Number of Features | 144 | 15 | 15 | 15 | 45 | 45 | 22 | 45 |
| Grass Healthy (85/178) | 0.00 | 0.00 | 0.00 | 55.06 | 0.00 | 0.00 | 0.00 | **84.26** |
| Grass Stressed (102/158) | 0.00 | 0.00 | 0.00 | 51.89 | 0.00 | 0.00 | **91.78** | 79.75 |
| Tree (89/70) | 0.00 | 0.00 | 0.00 | **100.00** | 0.00 | 0.00 | **100.00** | **100.00** |
| Residential (75/80) | 1.25 | 71.25 | **90.00** | 58.75 | 0.00 | 66.25 | 63.74 | 72.50 |
| Commercial (121/431) | 29.23 | 0.00 | 0.00 | 82.60 | 69.37 | 49.19 | 84.74 | **88.17** |
| Road (71/19) | 0.00 | 0.00 | 0.00 | **63.16** | 0.00 | 0.00 | 52.63 | 57.89 |
| Highway (92/326) | 0.00 | 51.23 | 0.00 | 46.63 | 15.34 | 23.93 | **76.07** | 63.19 |
| Railway (111/152) | 4.61 | 71.05 | 15.79 | 92.11 | 91.45 | 92.11 | **93.42** | 92.76 |
| Parking Lot 2 (27/20) | 5.00 | **10.00** | 0.00 | 5.00 | 0.00 | 0.00 | 0.00 | **10.00** |
| OA (%) | 9.42 | 22.31 | 6.70 | 66.71 | 34.96 | 34.54 | 71.97 | **79.84** |
| AA (%) | 4.45 | 22.61 | 11.75 | 61.56 | 20.52 | 36.60 | 62.49 | **71.95** |
| $\kappa$ | 0.160 | 0.134 | 0.111 | 0.679 | 0.206 | 0.230 | 0.717 | **0.784** |

**Accuracies for cloud-covered regions**

# Classification under shadow

| Features | $\text{Raw}_{hsi}$ | $Fspe$ | $Fspa$ | $Flid$ | $FEstacked$ | $Ffusion$ | $Fggf$ | Proposed |
|---|---|---|---|---|---|---|---|---|
| Number of Features | 144 | 15 | 15 | 15 | 45 | 45 | 22 | 45 |
| Grass Healthy (1053) | 82.15 | 81.77 | 82.72 | 57.93 | 82.81 | 83.00 | 82.91 | **97.34** |
| Grass Stressed (1064) | 82.05 | 82.24 | 76.22 | 60.90 | 83.36 | 83.74 | **99.44** | 95.58 |
| Grass Synthetis (505) | 99.80 | **99.80** | **100** | 94.85 | **100** | **100** | **100** | **100** |
| Tree (1056) | 92.90 | 89.20 | 83.62 | 76.23 | 92.42 | 91.48 | **99.24** | 97.44 |
| Soil (1056) | 97.92 | 98.58 | 98.30 | 83.14 | 99.43 | 99.81 | 99.81 | **99.83** |
| Water (143) | 95.10 | 95.10 | **99.30** | 84.62 | 95.80 | 95.80 | 95.80 | 95.80 |
| Residential (1072) | 76.31 | 78.82 | 83.68 | 82.65 | 85.26 | **97.11** | 91.42 | 97.01 |
| Commercial (1053) | 54.89 | 48.91 | 37.51 | **92.97** | 83.76 | 75.59 | 92.50 | 91.55 |
| Road (1931059) | 78.00 | 75.35 | 79.13 | 66.48 | 85.27 | 92.82 | 88.76 | **93.86** |
| Highway (1036) | 59.36 | 80.31 | 65.83 | 70.17 | 70.85 | 75.87 | 84.85 | **88.22** |
| Railway (1054) | 79.03 | 87.67 | 77.23 | 96.39 | 97.25 | **99.15** | 95.73 | 98.58 |
| Parking Lot 1 (1041) | 84.34 | 78.19 | 88.18 | 66.38 | 89.15 | 97.69 | 81.08 | **97.69** |
| Parking Lot 2 (285) | 72.28 | 71.58 | 72.63 | 63.86 | 80.00 | 77.89 | 74.39 | **82.46** |
| Tennis Court (247) | 99.60 | 99.60 | **100** | 99.60 | **100** | **100** | **100** | **100** |
| Running Track (473) | 97.25 | 97.04 | **100** | 58.35 | 98.52 | 98.73 | 98.73 | 98.73 |
| OA (%) | 80.78 | 81.96 | 79.70 | 75.82 | 88.16 | 90.44 | 92.05 | **95.81** |
| AA (%) | 83.40 | 84.29 | 82.96 | 76.97 | 89.55 | 91.25 | 92.31 | **95.60** |
| $\kappa$ | 0.793 | 0.805 | 0.779 | 0.738 | 0.871 | 0.896 | 0.914 | **0.954** |

**Accuracies for whole scene**

# Conclusion

- ✓ Compare different features for HS and LiDAR images
- ✓ Compare different fusion framework for fusion of HS and LiDAR data for classification
- ✓ Fusion of Hyperspectral and LiDAR Data for Classification of Cloud-Shadow Mixed Remote Sensed Scene

## Future works：

- Graph Convolutional Network and Label Propagation for Cross-domain classification
- Generative Adversarial Network for Multi-source Cross-domain Classification